

# Interference Exploitation in Full-Duplex Communications: Trading Interference Power for Both Uplink and Downlink Power Savings

Mahmoud T. Kabir<sup>1</sup>, *Student Member, IEEE*, Muhammad R. A. Khandaker<sup>2</sup>, *Senior Member, IEEE*, and Christos Masouros, *Senior Member, IEEE*

**Abstract**—This paper considers a multiuser full-duplex (FD) wireless communication system, where an FD radio base station (BS) serves multiple single-antenna half-duplex uplink and downlink users simultaneously. Unlike conventional interference mitigation approaches, we propose using knowledge of the data symbols and the channel state information (CSI) at the FD radio BS to exploit the multi-user interference constructively rather than to suppress it. We propose a multi-objective optimization problem (MOOP) via the weighted Tchebycheff method to study the tradeoff between the two desirable system design objectives, namely the total downlink transmit power and the total uplink transmit power, at the same time ensuring the required quality-of-service (QoS) for all users. In the proposed MOOP, we adapt the QoS constraints for the downlink users to accommodate constructive interference for both generic phase shift keying modulated signals and for quadrature amplitude modulated signals. We also extended our work to a robust design to study the system with imperfect uplink and downlink CSI. The simulation results and analysis show that significant power savings can be obtained. More importantly, however, the MOOP approach here allows for the power saved to be traded off for both uplink and downlink power savings, leading to an overall energy efficiency improvement in the wireless link.

**Index Terms**—Full-duplex, multi-objective optimization, constructive interference, power minimization, robust design.

## I. INTRODUCTION

THE high demand for improved spectrum-efficiency, power efficiency and guaranteed quality of service (QoS) in wireless links to meet the key requirements for the next generation 5G communications systems has brought full duplex (FD) at the forefront of research attention. Full duplex communications is widely recognized as one of the key technologies for 5G wireless communication systems [1].

Manuscript received September 18, 2017; revised September 18, 2018; accepted October 8, 2018. Date of publication October 23, 2018; date of current version December 10, 2018. This work was supported in part by the Engineering and Physical Sciences Research Council Project under Grant EP/R007934/1 and in part by the Petroleum Technology Development Fund through the Federal Republic of Nigeria. The associate editor coordinating the review of this paper and approving it for publication was L. Dai. (*Corresponding author: Mahmoud T. Kabir.*)

M. T. Kabir and C. Masouros are with the Department of Electronic and Electrical Engineering, University College London, London WC1E 7JE, U.K. (e-mail: kabir.tukur.15@ucl.ac.uk; c.masouros@ucl.ac.uk).

M. R. A. Khandaker is with the School of Engineering and Physical Sciences, Heriot-Watt University, Edinburgh EH14 4AS, U.K. (e-mail: m.khandaker@hw.ac.uk).

Color versions of one or more of the figures in this paper are available online at <http://ieeexplore.ieee.org>.

Digital Object Identifier 10.1109/TWC.2018.2876229

By allowing simultaneous transmission and reception, FD has the potential to drastically improve the spectral efficiency of the HD communication networks [2]–[5]. One major hurdle with the FD communication systems is the self-interference (SI) from the transmit antennas to the receive antennas of the wireless transceiver. This interference raises the noise floor and it becomes a dominant factor in the performance of the FD system. However, major breakthroughs have been made in practical FD system setups [2], [3] that show that the SI can be partially cancelled to within a few dB of the noise floor. While others focused on resource management, in [4], the authors investigated the spectral efficiency of FD small cell wireless systems by considering a joint beamformer design to maximize the spectral efficiency subject to power constraints. In [5], the authors used massive arrays at the FD relay station to cancel out loop interference and as a result increase the sum spectral efficiency of the system.

Many of the above FD solutions build upon existing beamforming solutions in the literature, that have been extensively developed for the downlink channel, moving from the sophisticated but capacity achieving non-linear beamforming techniques [6]–[8] to the less complex linear beamforming techniques [9]–[11]. Several optimization based schemes that provide optimal solutions subject to required quality of service (QoS) constraints have been proposed for multi-input single-output (MISO) systems in [12]. In [13], the authors addressed the problem of robust designs in downlink multi-user MISO systems with respect to erroneous channel state information (CSI). The work in [14] focused on addressing both max-min signal to noise and interference ratio balancing problem and power minimization problem with SINR constraints. More recently, it has been shown in [10], [11], and [15]–[17] that with the knowledge of the users' data symbols and the CSI, the interference can be classified into constructive and destructive interference. And further findings in [18]–[31] show that tremendous gains can be achieved by exploiting the constructive interference based on symbol level optimization for both PSK and QAM modulations. However, these findings are all based on MISO HD systems.

Our work extends the above interference exploitation concept to the FD transmission by employing multi-objective optimization, as most recently studied for FD in [32]–[34]. The authors in [32] investigated the power efficient resource

allocation for a MU-MIMO FD system. They proposed a multi-objective optimization problem (MOOP) to study the total uplink and downlink transmit power minimization problems jointly via the weighted Tchebycheff method. They extended their work to a robust and secure FD systems model in the presence of roaming users (eavesdroppers) in [33]. Similarly, in [34] the authors used a similar model to investigate the resource allocation for FD simultaneous wireless information and power transfer (SWIPT) systems. Accordingly, in this work we aim to further reduce the power consumption in FD MU-MIMO wireless communication systems by adopting the concept of constructive interference in the literature to the downlink channel for both PSK and QAM modulation. By exploiting the useful signal power from interference, we can provide a truly power efficient resource allocation for a FD MU-MIMO system. The interference exploitation concept is yet to be explored in the realm of FD transmission, where FD offers the unique opportunity to trade-off the harvested interference power for both uplink and downlink power savings through the MOOP designs.

We note that with regards to existing works in [18]–[31] on interference exploitation (IE), none of them consider FD transmission, and these works therefore are inapplicable to the scenario of interest. In fact, this paper is the first in the area of FD transmission to consider the exploitation of interference, where FD scenario brings unique challenges and opportunities to explore with respect to previous works on IE:

- The existence of self-interference (SI) introduces new constraints to the optimization problems, that change the power trade-offs involved.
- The trade-off between uplink and downlink power necessitates the study of MOOP, which is done for the first time here for IE, where previous works focused on single objective power minimization, SINR maximization etc.
- It is this joint optimization that brings, for the first time in the IE works, the opportunity to utilize constructive interference for uplink power savings. All existing works [18]–[31] exploit interference for downlink power savings only.
- The introduction of the SI and receive beamforming vectors in the optimization problems bring particular challenges to the robust optimization problems as will be shown later, which have resulted in new solvers with respect to both [32]–[34] and to existing robust solvers for IE [21].

However, with respect to the multi-objective optimization problems (MOOP) shown in [32] and [33] they focus on traditional interference rejection. In contrast, our work provides a step change in the MOOP considered, by introducing the concept of interference exploitation. As will be shown later, there is a clear distinction and particular performance gains with respect to the work in [32] and [33].

Against the state-of-the-art, we summarize our contributions below:

- 1) We first introduce the two FD system design objectives namely the total downlink transmit power and the total uplink transmit power. Then we formulate

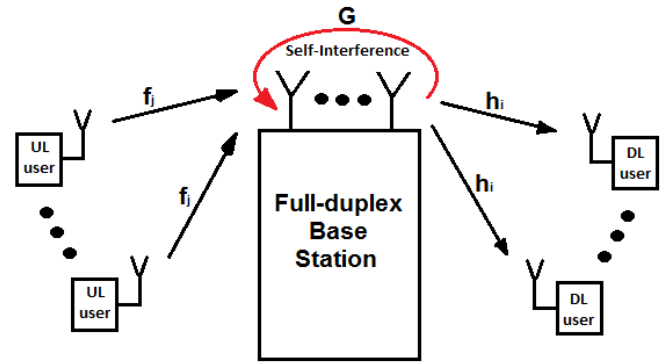


Fig. 1. System model with a FD radio BS with  $N$  antennas,  $K$  HD downlink users and  $J$  HD uplink users.

a MOOP to minimize the two objectives jointly via the weighted Tchebycheff method while exploiting the downlink interference for both uplink and downlink power savings.

- 2) By use of an auxiliary variable, we transform the proposed MOOP into a convex form, which can be efficiently solved using standard solvers.
- 3) We further derive robust MOOP for both the conventional and the proposed interference exploitation approach for erroneous uplink, downlink and SI channel CSI, where we consider the worst-case performance based on a deterministic model. We do this by recasting the MOOP into a virtual multicast problem and transforming it into a semidefinite program using slack variables.

The rest of the paper is organized as follows. Section II introduces the system model that is considered in this paper. Section III describes the conventional MOOP that minimizes the two system design objectives jointly. In Section IV, the proposed MOOP based on constructive interference regions are presented for PSK and QAM modulated symbols. Then in Section V, we present the robust versions of the MOOPs. In Section VI, we provide a computational complexity analysis of the MOOP formulations. Section VII illustrates the important results and discussions. And finally we conclude in Section VIII.

## II. SYSTEM MODEL

We consider a FD multiuser communication system as shown in Fig. 1. The system consists of a FD radio BS with  $N$  antennas serving  $K$  HD downlink users and  $J$  HD uplink users. Each user is equipped with a single antenna to reduce hardware complexity. Let  $\mathbf{h}_i \in \mathbb{C}^{N \times 1}$  be the channel vector between the FD radio BS and the  $i$ -th downlink user, and  $\mathbf{f}_j \in \mathbb{C}^{N \times 1}$  be the channel vector between the FD radio BS and the  $j$ -th uplink user. We denote the transmit signal vector from the FD radio BS to the  $i$ -th downlink user as

$$\mathbf{t}_i = \mathbf{w}_i d_i, \quad (1)$$

where  $\mathbf{w}_i \in \mathbb{C}^{N \times 1}$  and  $d_i$  denote the beamforming vector and the unit data symbol for the  $i$ -th downlink user. The received

signal at the  $i$ -th downlink user is:

$$y_i = \underbrace{\mathbf{h}_i^H \mathbf{t}_i}_{\text{desired signal}} + \underbrace{\sum_{k \neq i}^K \mathbf{h}_i^H \mathbf{t}_k}_{\text{interference plus noise}} + n_i, \quad (2)$$

where  $n_i \sim \mathcal{CN}(0, \sigma_i^2)$  represents the additive white Gaussian noise AWGN at the  $i$ -th downlink user. For each time slot the FD radio BS transmits  $K$  independent unit data symbols  $d$  simultaneously at the same frequency to the  $K$  downlink users. The first term in (2) represents the desired signal while the second term is the multiuser interference signal. For ease of exposition and since the uplink interference cannot be exploited in the style of interference exploitation that we present in this paper due to the absence of the knowledge of the uplink data at the FD BS, we neglect the uplink-to-downlink interference in our system model. In practice, this may be due to the weak uplink-to-downlink user channels due to physical obstructions and shadowing effects, or due to a dedicated overlaid interference avoidance scheme such as the one in [35]–[38]. Accordingly, the explicit interference terms can be avoided for simplicity, or assumed incorporated in the downlink users' noise term. We further note, however, that including the above interference in (2), would not change the proposed strategy in which we aim at exploiting the downlink interference power.

The received signal from the  $J$  uplink users at the FD radio BS is:

$$\mathbf{y}^{BS} = \sum_{j=1}^J \sqrt{P_j} \mathbf{f}_j x_j + \underbrace{\mathbf{G} \sum_{k=1}^K \mathbf{t}_k}_{\text{residual self-interference}} + \mathbf{z}, \quad (3)$$

where  $P_j$  and  $x_j$  denotes the uplink transmit power and the data symbol from the  $j$ -th uplink user respectively. The vector  $\mathbf{z} \sim \mathcal{CN}(0, \sigma_N^2)$  represents the additive white Gaussian noise AWGN at the FD radio BS. The matrix  $\mathbf{G} \in \mathbb{C}^{N \times N}$  denotes the self-interference (SI) channel. In the literature, different SI mitigation techniques have been proposed [39], [40] to reduce the effect of self-interference. In order to isolate our proposed scheme from the specific implementation of a SI mitigation technique, since the SI cannot be cancelled perfectly in FD systems due to limited dynamic range at the receiver even if the SI channel is known perfectly [33], [40]. We consider the worst-case performance based on deterministic model to model the residual-SI channel after cancellation. In essence, we assume the residual-SI channel  $\mathbf{G}$  to lie in the neighbourhood of the estimated channel. Hence, the actual channel due to imperfect SI channel estimate is given as

$$\mathbf{G} = \check{\mathbf{G}} + \Delta \mathbf{G}, \quad (4)$$

where  $\check{\mathbf{G}}$  denotes the SI channel estimate known to the FD BS and  $\Delta \mathbf{G}$  represents the SI channel uncertainties, which are assumed to be bounded such that  $\|\Delta \mathbf{G}\|^2 \leq \epsilon_G^2$ , for some  $\epsilon_G \geq 0$ . We assume the FD BS has no knowledge of  $\Delta \mathbf{G}$  only the error bound  $\epsilon_G$ .

Accordingly, the first term of (3) represents the desired signal from the  $j$ -th uplink user and the second term represents the residual SI signal. Before we formulate the problem, we first define the SINR at the  $i$ -th downlink user and at the FD radio BS respectively as (5) and (6), shown at the bottom of this page, where  $\mathbf{u}_j \in \mathbb{C}^{N \times 1}$  is the receive beamforming vector for detecting the received symbol from the  $j$ -th uplink user. In this paper, to reduce complexity, we adopt zero-forcing (ZF) beamforming at the FD BS for the detection of uplink signals. In this context, ZF beamforming is adopted since it provide a good trade-off between complexity and performance [41]. Hence, the receive beamforming vector for the  $j$ -th uplink user is given as

$$\mathbf{u}_j = (\mathbf{r}_j \mathbf{F}^\dagger)^H, \quad (7)$$

where  $\mathbf{r}_j = [0, \dots, 0, 1, 0, \dots, 0]$ ,  $\mathbf{F}^\dagger = (\mathbf{F}^H \mathbf{F})^{-1} \mathbf{F}^H$ ,  $\dagger$  denotes the pseudo-inverse operation and  $\mathbf{F} = [\mathbf{f}_1, \dots, \mathbf{f}_J]$ .

### III. CONVENTIONAL POWER MINIMIZATION PROBLEM

In this section, we study the conventional power minimization (PM) problem where all the interference are treated as undesired signals. We first introduce the two system design objectives, then we formulate a MOOP that aims to minimize the two objectives jointly.

In this section, we assume perfect channel state information (CSI) for the uplink and downlink channels. We focus on slow fading channel scenario, where the channels change at the beginning of each frame. Thus, to facilitate the channel realization in practice, handshaking is performed between the FD BS and all users. As the channel changes slowly, pilot signals are usually embedded in the data packets, which allows the FD BS to constantly update the CSI estimation of the transmission links of all users. Later in Section V, we explicitly treat imperfect CSI for designing a robust technique.

The two FD system design objectives are the total downlink transmit power

$$\sum_{i=1}^K \|\mathbf{w}_i\|^2, \quad \forall i, \quad (8)$$

and the total uplink transmit power

$$\sum_{j=1}^J P_j, \quad \forall j. \quad (9)$$

$$\text{SINR}_i^{DL} = \frac{|\mathbf{h}_i^H \mathbf{w}_i|^2}{\sum_{k \neq i}^K |\mathbf{h}_i^H \mathbf{w}_k|^2 + \sigma_i^2}, \quad (5)$$

$$\text{SINR}_j^{UL} = \frac{P_j |\mathbf{f}_j^H \mathbf{u}_j|^2}{\sum_{n \neq j}^J P_n |\mathbf{f}_n^H \mathbf{u}_j|^2 + \sum_{k=1}^K |\mathbf{u}_j^H (\check{\mathbf{G}} + \Delta \mathbf{G}) \mathbf{w}_k|^2 + \sigma_N^2 \|\mathbf{u}_j\|^2}, \quad (6)$$

These two objectives are very important to both the user and the system operator. In order to study these two objectives jointly, we formulate a MOOP. Multi-objective optimization is employed when there is a need to study jointly the trade-off between two desirable objectives via the concept of Pareto optimality. A point is said to be Pareto optimal if there is no other point that improves any of the objectives without decreasing the others [42]. In [42], a survey of multi-objective optimization methods in engineering applications was presented. By using the weighted Tchebycheff method [42], which can achieve the complete Pareto optimal set with lower computational complexity, the MOOP that aims to minimize the total downlink and uplink transmit power jointly for the considered FD system is typically formulated as [32] and [33]

$$\begin{aligned} \mathcal{P}1 : \quad & \min_{\mathbf{w}_i, P_j} \max_{a=1,2} \{ \lambda_a (R_a^* - R_a) \} \\ \text{s.t. A1} : \quad & \frac{|\mathbf{h}_i^H \mathbf{w}_i|^2}{\sum_{k \neq i}^K |\mathbf{h}_i^H \mathbf{w}_k|^2 + \sigma_i^2} \geq \Gamma_i^{DL}, \quad \forall i, \\ \text{A2} : \quad & \frac{P_j |\mathbf{f}_j^H \mathbf{u}_j|^2}{I_j + \sigma_N^2 \|\mathbf{u}_j\|^2} \geq \Gamma_j^{UL}, \quad \forall \|\Delta \mathbf{G}\|^2 \leq \epsilon_G^2, \quad \forall j, \end{aligned} \quad (10)$$

where,  $I_j = \sum_{n \neq j}^J P_n |\mathbf{f}_n^H \mathbf{u}_j|^2 + \sum_{k=1}^K |\mathbf{u}_j^H (\tilde{\mathbf{G}} + \Delta \mathbf{G}) \mathbf{w}_k|^2$ . We define  $\Gamma_i^{DL}$  and  $\Gamma_j^{UL}$  as the minimum required SINRs for the  $i$ -th downlink user and the  $j$ -th uplink user, respectively. We denote  $R_1 = \sum_{i=1}^K \|\mathbf{w}_i\|^2$  and  $R_2 = \sum_{j=1}^J P_j$  as the two system design objectives, respectively.  $R_1^*$  and  $R_2^*$  are the optimal values of the two system design objectives in the downlink and uplink, respectively. The variable  $\lambda_a \geq 0$ ,  $\sum \lambda_a = 1$ , specifies the priority given to the  $a$ -th objective i.e. for a given  $\lambda_1 = 0.8$  means 80% priority is given to  $R_1$  and 20% priority to  $R_2$ , respectively. By varying  $\lambda_a$  we can obtain the complete Pareto optimal set.

Problem  $\mathcal{P}1$  is a non-convex problem due to the SINR constraints A1 and A2, and it is commonly solved via semidefinite relaxation as in [32] and [33].

#### IV. POWER MINIMIZATION PROBLEM BASED ON CONSTRUCTIVE INTERFERENCE

In this section, we study the power minimization (PM) optimization problems based on constructive interference. With prior knowledge of the CSI and users' data symbols for the downlink users, the instantaneous interference can be exploited rather than suppressed [21]. To be precise, constructive interference is the interference that pushes the received signal further into the detection region of the constellation and away from the detection threshold [21]. This concept has been thoroughly studied in the literature for both PSK and Multi-Level Adaptive modulation [19]. We refer the reader to [18], [20], and [21] for further details of this topic. Motivated by this idea, here, we apply this concept to the PM problem in Section III for both PSK and QAM modulated symbols. We note that constructive interference is only applied to the downlink users and not the uplink users

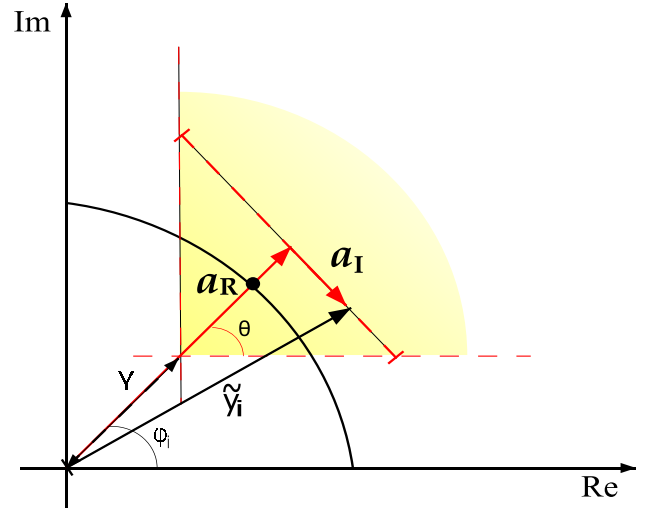


Fig. 2. Constructive interference region for a QPSK constellation point.

following that only the prior knowledge of the CSI and users' data symbols for the downlink users are available at the BS. Nevertheless, we show in the following that power savings can be obtained for both uplink and downlink transmission, by means of the MOOP design.

#### A. Constructive Interference for PSK Modulation

To illustrate this concept, we provide a geometric illustration of the constructive interference regions for a QPSK constellation in Fig. 2. First, we can define the total downlink transmit signal vector as

$$\sum_{k=1}^K \mathbf{w}_k d_k = \sum_{k=1}^K \mathbf{w}_k e^{j(\phi_k - \phi_i)} d_i, \quad (11)$$

where  $d_i = d e^{j\phi_i}$  is the desired symbol for the  $i$ -th downlink user. Therefore, the received signal (2) without noise at the  $i$ -th downlink user can be defined as

$$\tilde{y}_i = \mathbf{h}_i^H \sum_{k=1}^K \mathbf{w}_k d_k, \quad (12)$$

$$= \mathbf{h}_i^H \sum_{k=1}^K \mathbf{w}_k e^{j(\phi_k - \phi_i)} d_i, \quad (13)$$

Accordingly, since the interference contributes constructively to the received signal, it has been shown in [11] that the downlink SNR at the  $i$ -th downlink user (5) can be rewritten as

$$\text{SNR}_i^{DL} = \frac{|\mathbf{h}_i^H \sum_{k=1}^K \mathbf{w}_k d_k|^2}{\sigma_i^2}. \quad (14)$$

Without loss of generality, by taking user 1 as reference the instantaneous downlink transmit power for a unit symbol is

$$P_{total} = \left\| \sum_{k=1}^K \mathbf{w}_k e^{j(\phi_k - \phi_1)} \right\|^2. \quad (15)$$

As detailed in [21], the shaded area in Fig. 2 is the region of constructive interference. If the received signal  $\tilde{y}_i$  falls within this region, then interference has been exploited constructively. The angle  $\theta = \pm \frac{\pi}{M}$  determines the maximum angle shift of the constructive interference region for a modulation order  $M$ ,  $a_I$  and  $a_R$  are the imaginary and real parts of the received signal  $\tilde{y}_i$  without the noise, respectively. The detection threshold is determined by  $\gamma = \sqrt{\Gamma_i^{DL} \sigma_i^2}$ .

Therefore, by applying these definitions and basic geometry from Fig. 2 it can be seen that for the received signal to fall in the constructive region of the constellation we need to have  $a_I \leq (a_R - \gamma) \tan \theta$ . Accordingly, we can define the downlink SINR constraint that guarantees constructive interference at the  $i$ -th downlink user by

$$\begin{aligned} & \left| \text{Im} \left( \mathbf{h}_i^H \sum_{k=1}^K \mathbf{w}_k e^{j(\phi_k - \phi_i)} \right) \right| \\ & \leq \left( \text{Re} \left( \mathbf{h}_i^H \sum_{k=1}^K \mathbf{w}_k e^{j(\phi_k - \phi_i)} \right) - \sqrt{\Gamma_i^{DL} \sigma_i^2} \right) \tan \theta. \end{aligned} \quad (16)$$

Based on the analysis above, we can modify the SINR constraints for the downlink users in the conventional MOOP to accommodate for CI. Thus, the CI-based MOOP for MPSK modulated symbols is expressed as

$$\begin{aligned} \mathcal{P}2: \quad & \min_{\mathbf{w}_i, P_j, t} t \\ \text{s.t. B1:} \quad & \left| \text{Im} \left( \mathbf{h}_i^H \sum_{k=1}^K \mathbf{w}_k e^{j(\phi_k - \phi_i)} \right) \right| \\ & \leq \left( \text{Re} \left( \mathbf{h}_i^H \sum_{k=1}^K \mathbf{w}_k e^{j(\phi_k - \phi_i)} \right) - \sqrt{\Gamma_i^{DL} \sigma_i^2} \right) \\ & \tan \theta, \quad \forall i, \\ \text{B2:} \quad & \frac{P_j |\mathbf{f}_j^H \mathbf{u}_j|^2}{I_j^{PSK} + \left| \sum_{k=1}^K \mathbf{u}_j^H (\check{\mathbf{G}} + \Delta \mathbf{G}) \mathbf{w}_k e^{j(\phi_k - \phi_1)} \right|^2} \\ & \geq \Gamma_j^{UL}, \\ & \forall \|\Delta \mathbf{G}\|^2 \leq \epsilon_G^2, \quad \forall j, \\ \text{B3:} \quad & \lambda_a (R_a^* - R_a) \leq t, \quad \forall a \in \{1, 2\}, \end{aligned} \quad (17)$$

where,  $t$  is an auxiliary variable and  $I_j^{PSK} = \sum_{n \neq j} P_n |\mathbf{f}_n^H \mathbf{u}_j|^2 + \sigma_N^2 \|\mathbf{u}_j\|^2$ .

Here  $R_1 = \left\| \sum_{k=1}^K \mathbf{w}_k e^{j(\phi_k - \phi_1)} \right\|^2$  and  $R_2 = \sum_{j=1}^J P_j$ . Unlike its conventional counterpart, constraint A1, it can be seen that constraint B1 is convex. However, constraint B2 is not convex due to channel uncertainties in the SI term. To transform B2 into a convex constraint, we rewrite B2 as the following two constraints by introducing a slack variable

$S_j^{SI} > 0, \forall j$ , respectively,

$$P_j |\mathbf{f}_j^H \mathbf{u}_j|^2 - \Gamma_j^{UL} \left( \sum_{n \neq j} P_n |\mathbf{f}_n^H \mathbf{u}_j|^2 + S_j^{SI} + \sigma_N^2 \|\mathbf{u}_j\|^2 \right) \geq 0, \quad \forall j, \quad (18)$$

$$\left| \sum_{k=1}^K \mathbf{u}_j^H (\check{\mathbf{G}} + \Delta \mathbf{G}) \mathbf{w}_k e^{j(\phi_k - \phi_1)} \right|^2 \leq S_j^{SI}, \quad \forall \|\Delta \mathbf{G}\|^2 \leq \epsilon_G^2, \quad \forall j. \quad (19)$$

Notice that (19) can be guaranteed by the following modified constraint

$$\max_{\|\Delta \mathbf{G}\|^2 \leq \epsilon_G^2} \left| \sum_{k=1}^K \mathbf{u}_j^H (\check{\mathbf{G}} + \Delta \mathbf{G}) \mathbf{w}_k e^{j(\phi_k - \phi_1)} \right|^2 \leq S_j^{SI}, \quad \forall j. \quad (20)$$

By using the fact that  $\|\mathbf{x} + \mathbf{y}\|^2 \leq (\|\mathbf{x}\| + \|\mathbf{y}\|)^2$ , (20) can always be guaranteed by the following constraint, (21), shown at the bottom of this page, whose worst-case formulation is given by

$$\left( \left| \sum_{k=1}^K \mathbf{u}_j^H \check{\mathbf{G}} \mathbf{w}_k e^{j(\phi_k - \phi_1)} \right| + \epsilon_G \left| \sum_{k=1}^K \mathbf{u}_j^H \mathbf{w}_k e^{j(\phi_k - \phi_1)} \right| \right)^2 \leq S_j^{SI}, \quad \forall j. \quad (22)$$

Therefore, the transformed problem  $\mathcal{P}2$  is given by

$$\begin{aligned} \widetilde{\mathcal{P}2}: \quad & \min_{\mathbf{w}_i, P_j, t} t \\ \text{s.t. B1:} \quad & \left| \text{Im} \left( \mathbf{h}_i^H \sum_{k=1}^K \mathbf{w}_k e^{j(\phi_k - \phi_i)} \right) \right| \\ & \leq \left( \text{Re} \left( \mathbf{h}_i^H \sum_{k=1}^K \mathbf{w}_k e^{j(\phi_k - \phi_i)} \right) - \sqrt{\Gamma_i^{DL} \sigma_i^2} \right) \tan \theta, \quad \forall i, \\ \widetilde{\text{B2a:}} \quad & P_j |\mathbf{f}_j^H \mathbf{u}_j|^2 \\ & - \Gamma_j^{UL} \left( \sum_{n \neq j} P_n |\mathbf{f}_n^H \mathbf{u}_j|^2 + S_j^{SI} + \sigma_N^2 \|\mathbf{u}_j\|^2 \right) \geq 0, \quad \forall j, \\ \widetilde{\text{B2b:}} \quad & \left( \left| \sum_{k=1}^K \mathbf{u}_j^H \check{\mathbf{G}} \mathbf{w}_k e^{j(\phi_k - \phi_1)} \right| + \epsilon_G \left| \sum_{k=1}^K \mathbf{u}_j^H \mathbf{w}_k e^{j(\phi_k - \phi_1)} \right| \right)^2 \\ & \leq S_j^{SI}, \quad \forall j, \\ \text{B3:} \quad & \lambda_a (R_a^* - R_a) \leq t, \quad \forall a \in \{1, 2\}. \end{aligned} \quad (23)$$

The problem  $\widetilde{\mathcal{P}2}$  is now jointly convex with respect to the optimization variables, since constraint B1 is a standard second-order cone constraint,  $\widetilde{\text{B2a}}$  is a linear constraint and  $\widetilde{\text{B2b}}$  is a quadratic constraint. Hence,  $\widetilde{\mathcal{P}2}$  can be efficiently solved using standard solvers like CVX [43].

$$\max_{\|\Delta \mathbf{G}\|^2 \leq \epsilon_G^2} \left( \left| \sum_{k=1}^K \mathbf{u}_j^H \check{\mathbf{G}} \mathbf{w}_k e^{j(\phi_k - \phi_1)} \right| + \left| \sum_{k=1}^K \mathbf{u}_j^H \Delta \mathbf{G} \mathbf{w}_k e^{j(\phi_k - \phi_1)} \right| \right)^2 \leq S_j^{SI}, \quad \forall j, \quad (21)$$

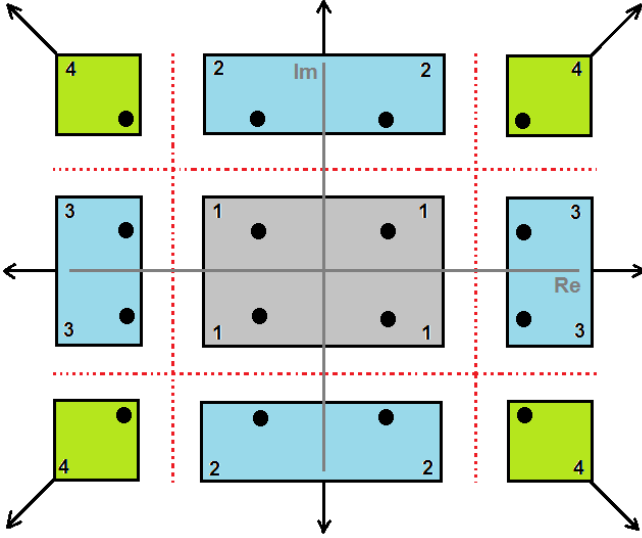


Fig. 3. Schematic representation of 16QAM constellation points.

Now we highlight the main advantage of the proposed optimization problem over the conventional optimization problem in Section III. In the optimization problem in Section III, the constraints suppress the interference each user experience, which is equivalent to constraining the interference such that the signal received is just within the nominal constellation point. While in the case of proposed optimization problem  $\mathcal{P}2$ , constraint B1 relaxes the optimization and allows for a larger detection region as shown in Fig. 2. Hence, this translates to a larger feasible solution set thereby leading to reduction in the total transmit power as compared to the conventional optimization problem in Section III, which will be demonstrated later through simulation results.

### B. Constructive Interference for QAM Modulation

To illustrate the concept of constructive interference for QAM modulation we provide a schematic representation for 16QAM constellation points in Fig. 3. Based on [44], to guarantee constructive interference for the constellation points, we rewrite the SINR constraints for the downlink users to exploit the specific detection regions for each group of constellation points separately as detailed below. First, we redefine the received signal without noise at the  $i$ -th downlink user as in (12) and the instantaneous downlink transmit power (14) in terms of amplitude not phase as

$$P_{total} = \left\| \sum_{k=1}^K \mathbf{w}_k d_k \right\|^2. \quad (24)$$

From Fig. 3, to ensure constructive interference is achieved and the constellation points are received in the correct detection region for the downlink users, the following constraints are adopted. Note that the dotted lines in Fig. 3 represent the decision boundaries.

- For the group of constellation points in the box labelled “1” in Fig. 3, since they are all surrounded by the decision

boundaries, the constraints should guarantee that the received signals achieve the exact constellation point so as not to exceed the decision boundaries. The constraints are

$$C1 : \text{Re}(\tilde{y}_i) = \sqrt{\Gamma_i^{DL}} \sigma_i \text{Re}(d_i),$$

$$C2 : \text{Im}(\tilde{y}_i) = \sqrt{\Gamma_i^{DL}} \sigma_i \text{Im}(d_i).$$

- For the group of constellation points labelled “2” in Fig. 3, the constraints should guarantee that the received signals fall in the detection region away from the decision boundaries, which is the real axis. The constraints are

$$C1 : \text{Re}(\tilde{y}_i) = \sqrt{\Gamma_i^{DL}} \sigma_i \text{Re}(d_i),$$

$$C2 : \text{Im}(\tilde{y}_i) \geq \sqrt{\Gamma_i^{DL}} \sigma_i \text{Im}(d_i).$$

- For the group of constellation points labelled “3” in Fig. 3, the constraints should guarantee that the received signals fall in the detection region away from the decision boundaries, which is the imaginary axis. The constraints are

$$C1 : \text{Re}(\tilde{y}_i) \geq \sqrt{\Gamma_i^{DL}} \sigma_i \text{Re}(d_i),$$

$$C2 : \text{Im}(\tilde{y}_i) = \sqrt{\Gamma_i^{DL}} \sigma_i \text{Im}(d_i).$$

- For the group of constellation points labelled “4” in Fig. 3, the constraints should guarantee that the received signals fall in the detection region away from the decision boundaries. Here, the constellation points are not surrounded by the decision boundaries and therefore have a larger detection region that extend infinitely. The constraints are

$$C1 : \text{Re}(\tilde{y}_i) \geq \sqrt{\Gamma_i^{DL}} \sigma_i \text{Re}(d_i),$$

$$C2 : \text{Im}(\tilde{y}_i) \geq \sqrt{\Gamma_i^{DL}} \sigma_i \text{Im}(d_i).$$

By adopting the required downlink SINR constraints C1 and C2 for the corresponding group constellation points, the conventional MOOP can be modified to accommodate for CI. Therefore, the CI-based MOOP for 16QAM modulation can be expressed as

$$\begin{aligned} \mathcal{P}3 : \min_{\mathbf{w}_i, P_j, t} \quad & t \\ \text{s.t.} \quad & \text{Constraints C1 and C2, } \forall i, \\ & C3a : P_j |\mathbf{f}_j^H \mathbf{u}_j|^2 \\ & \quad - \Gamma_j^{UL} \left( \sum_{n \neq j}^J P_n |\mathbf{f}_n^H \mathbf{u}_j|^2 + S_j^{SI} + \sigma_N^2 \|\mathbf{u}_j\|^2 \right) \\ & \geq 0, \quad \forall j, \\ & C3b : \left( \left| \sum_{k=1}^K \mathbf{u}_j^H \tilde{\mathbf{G}} \mathbf{w}_k d_k \right| + \epsilon_G \left| \sum_{k=1}^K \mathbf{u}_j^H \mathbf{w}_k d_k \right| \right)^2 \\ & \leq S_j^{SI}, \quad \forall j, \\ & C4 : \lambda_a (R_a^* - R_a) \leq t, \quad \forall a \in \{1, 2\}. \end{aligned} \quad (25)$$

where,  $R_1 = \left\| \sum_{k=1}^K \mathbf{w}_k d_k \right\|^2$  and  $R_2 = \sum_{j=1}^J P_j$ .

Again, it can be observed that unlike their conventional counterparts,  $\mathcal{P}3$  above is jointly convex with respect to the

optimization variables and can be optimally solved using standard convex solvers like CVX [43].

## V. MULTI-OBJECTIVE OPTIMIZATION PROBLEM WITH IMPERFECT CSI

### A. Conventional Robust MOOP

In this section we study the robustness of the system when the downlink and the uplink CSI are not perfectly known. There are two approaches frequently used to model or characterize imperfect CSI: the probabilistic approach and the deterministic approach. In probabilistic approach, the error in the CSI knowledge is assumed to have a certain statistical characteristic like the mean or covariance of the channel. In deterministic approach, which is adopted in this Section, the error in the CSI is assumed to belong to a given uncertainty set. The size of the set determines the amount of uncertainty on the channel and the system optimizes the worst-case performance which achieves a guaranteed performance level for any channel realization in the set. Therefore, for convenience and to avoid any statistical assumptions on the channel, we adopt the deterministic approach which corresponds well to quantization errors and is also suitable for handling slow-fading channels [45]. Thus, for each user, their actual channel is modeled as

$$\mathbf{h}_i = \check{\mathbf{h}}_i + \Delta \mathbf{h}_i, \quad \forall i, \quad (26)$$

$$\mathbf{f}_j = \check{\mathbf{f}}_j + \Delta \mathbf{f}_j, \quad \forall j, \quad (27)$$

where  $\check{\mathbf{h}}_i$  and  $\check{\mathbf{f}}_j$  denote the downlink and the uplink CSI estimates known to the FD BS, respectively. And  $\Delta \mathbf{h}_i, \forall i$  and  $\Delta \mathbf{f}_j, \forall j$  represent the downlink and the uplink CSI uncertainties, respectively, which are assumed to be bounded such that

$$\|\Delta \mathbf{h}_i\|^2 \leq \epsilon_{h,i}^2, \text{ for some } \epsilon_{h,i} \geq 0, \quad (28)$$

$$\|\Delta \mathbf{f}_j\|^2 \leq \epsilon_{f,j}^2, \text{ for some } \epsilon_{f,j} \geq 0. \quad (29)$$

We assume that the FD BS has no knowledge of  $\Delta \mathbf{h}_i$  and  $\Delta \mathbf{f}_j$  except for their error bounds, hence, we take the worst-case approach for our problem design. Thus, the MOOP formulation of  $\mathcal{P}1$  with imperfect CSI is

$$\begin{aligned} \mathcal{P}4: \min_{\mathbf{w}_i, P_j, t} \quad & t \\ \text{s.t. D1: } \quad & \frac{\left| (\check{\mathbf{h}}_i + \Delta \mathbf{h}_i)^H \mathbf{w}_i \right|^2}{\sum_{k \neq i}^K \left| (\check{\mathbf{h}}_i + \Delta \mathbf{h}_i)^H \mathbf{w}_k \right|^2 + \sigma_i^2} \geq \Gamma_i^{DL}, \\ & \forall \|\Delta \mathbf{h}_i\|^2 \leq \epsilon_{h,i}^2, \quad \forall i, \\ \text{D2: } \quad & \frac{P_j \left| (\check{\mathbf{f}}_j + \Delta \mathbf{f}_j)^H \mathbf{u}_j \right|^2}{\sum_{n \neq j}^J P_n \left| (\check{\mathbf{f}}_n + \Delta \mathbf{f}_n)^H \mathbf{u}_j \right|^2 + C_j} \geq \Gamma_j^{UL}, \\ & \forall \|\Delta \mathbf{G}\|^2 \leq \epsilon_G^2, \forall \|\Delta \mathbf{f}_j\|^2 \leq \epsilon_{f,j}^2, \quad \forall j, \\ \text{D3: } \quad & \lambda_a (R_a^* - R_a) \leq t, \quad \forall a \in \{1, 2\}. \end{aligned} \quad (30)$$

where  $C_j = \sum_{k=1}^K \left| \mathbf{u}_j^H (\check{\mathbf{G}} + \Delta \mathbf{G}) \mathbf{w}_k \right|^2 + \sigma_N^2 \|\mathbf{u}_j\|^2$

In the downlink and uplink SINR constraints, there are infinitely many inequalities which make the worst-case design

particularly challenging. To make  $\mathcal{P}4$  more tractable, we formulate the problem as a semidefinite program (SDP) then transform the constraints into linear matrix inequalities (LMI), which can be efficiently solved by existing solvers like CVX [43]. The SDP transformation of problem  $\mathcal{P}4$  is given by

$$\begin{aligned} \min_{\mathbf{w}_i, P_j, t} \quad & t \\ \text{s.t. } \widetilde{\text{D1}}: \quad & \frac{(\check{\mathbf{h}}_i + \Delta \mathbf{h}_i)^H \mathbf{W}_i (\check{\mathbf{h}}_i + \Delta \mathbf{h}_i)}{\sum_{k \neq i}^K ((\check{\mathbf{h}}_i + \Delta \mathbf{h}_i)^H \mathbf{W}_k (\check{\mathbf{h}}_i + \Delta \mathbf{h}_i)) + \sigma_i^2} \geq \Gamma_i^{DL}, \\ & \forall \|\Delta \mathbf{h}_i\|^2 \leq \epsilon_{h,i}^2, \quad \forall i, \\ \widetilde{\text{D2}}: \quad & \frac{P_j (\check{\mathbf{f}}_j + \Delta \mathbf{f}_j)^H \mathbf{U}_j (\check{\mathbf{f}}_j + \Delta \mathbf{f}_j)}{\sum_{n \neq j}^J P_n (\check{\mathbf{f}}_n + \Delta \mathbf{f}_n)^H \mathbf{U}_j (\check{\mathbf{f}}_n + \Delta \mathbf{f}_n) + \tilde{C}_j} \\ & \geq \Gamma_j^{UL}, \\ & \forall \|\Delta \mathbf{G}\|^2 \leq \epsilon_G^2, \forall \|\Delta \mathbf{f}_j\|^2 \leq \epsilon_{f,j}^2, \quad \forall j, \\ \widetilde{\text{D3}}: \quad & \lambda_a (R_a^* - R_a) \leq t, \quad \forall a \in \{1, 2\}. \\ \widetilde{\text{D4}}: \quad & \mathbf{W}_i \succeq 0, \quad \forall i. \end{aligned} \quad (31)$$

where,

$$\tilde{C}_j = \text{Tr} \left\{ (\check{\mathbf{G}} + \Delta \mathbf{G}) \sum_{k=1}^K \mathbf{W}_k (\check{\mathbf{G}} + \Delta \mathbf{G})^H \mathbf{U}_j \right\} + \sigma_N^2 \text{Tr} \{ \mathbf{U}_j \}$$

and we define  $\mathbf{W}_i = \mathbf{w}_i \mathbf{w}_i^H$  and  $\mathbf{U}_j = \mathbf{u}_j \mathbf{u}_j^H$ .

Next, we can rearrange constraint  $\widetilde{\text{D1}}$  into

$$\begin{aligned} (\check{\mathbf{h}}_i + \Delta \mathbf{h}_i)^H \mathbf{Q}_i (\check{\mathbf{h}}_i + \Delta \mathbf{h}_i) - \Gamma_i^{DL} \sigma_i^2 \geq 0, \\ \forall \|\Delta \mathbf{h}_i\|^2 \leq \epsilon_{h,i}^2, \quad \forall i. \end{aligned} \quad (32)$$

where, we introduce

$$\mathbf{Q}_i \triangleq \mathbf{W}_i - \Gamma_i^{DL} \sum_{k \neq i}^K \mathbf{W}_k, \quad \forall i$$

and then for constraint  $\widetilde{\text{D2}}$ , let's define two vectors  $\tilde{\mathbf{f}}$  and  $\tilde{\Delta \mathbf{f}}$  as

$$\tilde{\mathbf{f}} = \begin{bmatrix} \check{\mathbf{f}}_1 \\ \vdots \\ \check{\mathbf{f}}_J \end{bmatrix} \in \mathbb{C}^{NJ \times 1}, \quad \tilde{\Delta \mathbf{f}} = \begin{bmatrix} \Delta \mathbf{f}_1 \\ \vdots \\ \Delta \mathbf{f}_J \end{bmatrix} \in \mathbb{C}^{NJ \times 1}. \quad (33)$$

Hence, we can define any  $\check{\mathbf{f}}_j = \mathbf{B}_j \tilde{\mathbf{f}}$  and  $\Delta \mathbf{f}_j = \mathbf{B}_j \tilde{\Delta \mathbf{f}}$ , for  $j = 1, \dots, J$ , with  $\mathbf{B}_j \in \mathbb{R}^{N \times NJ}$  defined as  $\mathbf{B}_j = [\mathbf{B}_{j,1}, \dots, \mathbf{B}_{j,J}]$ , where  $\mathbf{B}_{j,j} = \mathbf{I}_N$  and  $\mathbf{B}_{j,n} = \mathbf{0}_N$ , for  $n = 1, \dots, J, n \neq j$ . We have  $\mathbf{I}_N$  and  $\mathbf{0}_N$  to be an  $N \times N$  identity matrix and zero matrix, respectively. Now constraint  $\widetilde{\text{D2}}$  can be rewritten as

$$\begin{aligned} \frac{P_j \left( (\mathbf{B}_j \tilde{\mathbf{f}} + \mathbf{B}_j \tilde{\Delta \mathbf{f}})^H \mathbf{U}_j (\mathbf{B}_j \tilde{\mathbf{f}} + \mathbf{B}_j \tilde{\Delta \mathbf{f}}) \right)}{\sum_{n \neq j}^J P_n \left( (\mathbf{B}_n \tilde{\mathbf{f}} + \mathbf{B}_n \tilde{\Delta \mathbf{f}})^H \mathbf{U}_j (\mathbf{B}_n \tilde{\mathbf{f}} + \mathbf{B}_n \tilde{\Delta \mathbf{f}}) \right) + \tilde{C}_j} \\ \geq \Gamma_j^{UL}, \quad \forall \|\Delta \mathbf{G}\|^2 \leq \epsilon_G^2, \quad \forall \|\tilde{\Delta \mathbf{f}}\|^2 \leq \epsilon_f^2, \quad \forall j, \end{aligned} \quad (34)$$



by randomization technique as in [48], such that  $\mathbf{W}_i = \mathbf{w}_i \mathbf{w}_i^H, \forall i$ . Let

### B. Robust MOOP Based on CI for MPSK Modulation

To study the robustness of the proposed system based on constructive interference, for notational simplicity, we formulate  $\widetilde{\mathcal{P}}2$  as a virtual multicast problem. The motivation for recasting  $\widetilde{\mathcal{P}}2$  into a virtual multicast problem is for the ease of transforming the robust CI based MOOP into convex form. As the constraint B1 in the problem  $\widetilde{\mathcal{P}}2$  involves dealing with real and imaginary parts of the received signal ( $\widetilde{y}_i$ ) separately, analysis will be easier with real valued numbers, hence, the need for virtual multicast formulation. To facilitate this, we simply incorporate each user's channel with its respective data symbol i.e.  $\widetilde{\mathbf{h}}_i = \mathbf{h}_i e^{j(\phi_1 - \phi_i)}$  and let  $\mathbf{w} = \sum_{k=1}^K \mathbf{w}_k e^{j(\phi_k - \phi_1)}$ . Following this the multicast formulation of problem  $\widetilde{\mathcal{P}}2$  can be written as

$$\begin{aligned} \mathcal{P}6: \min_{\mathbf{w}, P_j, t} & t \\ \text{s.t.} & \left| \text{Im} \left( \widetilde{\mathbf{h}}_i^H \mathbf{w} \right) \right| \leq \left( \text{Re} \left( \widetilde{\mathbf{h}}_i^H \mathbf{w} \right) - \sqrt{\Gamma_i^{DL} \sigma_i^2} \right) \tan \theta, \\ & \forall i, \frac{P_j |\mathbf{f}_j^H \mathbf{u}_j|^2}{\sum_{n \neq j} P_n |\mathbf{f}_n^H \mathbf{u}_j|^2 + |\mathbf{u}_j^H \mathbf{G} \mathbf{w}|^2 + \sigma_N^2 \|\mathbf{u}_j\|^2} \\ & \geq \Gamma_j^{UL}, \quad \forall j, \\ & \lambda_a (R_a^* - R_a) \leq t, \quad \forall a \in \{1, 2\}. \end{aligned} \quad (42)$$

Based on the multicast formulation  $\mathcal{P}6$ , for the worst-case design we model the imperfect CSI as

$$\widetilde{\mathbf{h}}_i = \check{\mathbf{h}}_i + \Delta \widetilde{\mathbf{h}}_i, \quad \forall i, \quad (43)$$

where  $\check{\mathbf{h}}_i$  denotes the downlink CSI estimate known to the FD BS and  $\Delta \widetilde{\mathbf{h}}_i$  is the downlink CSI uncertainty which is bounded such that  $\|\Delta \widetilde{\mathbf{h}}_i\|^2 \leq \epsilon_{h,i}^2$ . Similarly, we model the uplink CSI as in Section V-A. The robust formulation of problem  $\mathcal{P}6$  is

$$\begin{aligned} \mathcal{P}7: \min_{\mathbf{w}, P_j, t} & t \\ \text{s.t.} & \left| \text{Im} \left( (\check{\mathbf{h}}_i + \Delta \widetilde{\mathbf{h}}_i)^H \mathbf{w} \right) \right| \\ & \leq \left( \text{Re} \left( (\check{\mathbf{h}}_i + \Delta \widetilde{\mathbf{h}}_i)^H \mathbf{w} \right) - \sqrt{\Gamma_i^{DL} \sigma_i^2} \right) \tan \theta, \\ & \forall \|\Delta \widetilde{\mathbf{h}}_i\|^2 \leq \epsilon_{h,i}^2, \quad \forall i, \\ & \frac{P_j |(\check{\mathbf{f}}_j + \Delta \widetilde{\mathbf{f}}_j)^H \mathbf{u}_j|^2}{\sum_{n \neq j} P_n |(\check{\mathbf{f}}_n + \Delta \widetilde{\mathbf{f}}_n)^H \mathbf{u}_j|^2 + I_j} \geq \Gamma_j^{UL}, \\ & \forall \|\Delta \mathbf{G}\|^2 \leq \epsilon_G^2, \quad \forall \|\Delta \mathbf{f}_j\|^2 \leq \epsilon_{f,j}^2, \quad \forall j, \\ & \lambda_a (R_a^* - R_a) \leq t, \quad \forall a \in \{1, 2\}. \end{aligned} \quad (44)$$

where  $I_j = |\mathbf{u}_j^H (\check{\mathbf{G}} + \Delta \mathbf{G}) \mathbf{w}|^2 + \sigma_N^2 \|\mathbf{u}_j\|^2$ .

First, let's consider the downlink SINR constraint. For convenience we separate the real and imaginary part of the complex notations and represent them as real valued numbers.

$$\underline{\mathbf{w}} \triangleq \begin{bmatrix} \text{Re}(\mathbf{w}) \\ \text{Im}(\mathbf{w}) \end{bmatrix}, \quad (45)$$

$$\check{\mathbf{h}}_i \triangleq [\text{Im}(\check{\mathbf{h}}_i)^H \quad \text{Re}(\check{\mathbf{h}}_i)^H], \quad (46)$$

$$\Delta \widetilde{\mathbf{h}}_i \triangleq [\text{Im}(\Delta \widetilde{\mathbf{h}}_i)^H \quad \text{Re}(\Delta \widetilde{\mathbf{h}}_i)^H], \quad (47)$$

$$\mathbf{\Pi} \triangleq \begin{bmatrix} \mathbf{0}_N & -\mathbf{I}_N \\ \mathbf{I}_N & \mathbf{0}_N \end{bmatrix}. \quad (48)$$

where,  $\mathbf{0}_N$  and  $\mathbf{I}_N$  denote  $N \times N$  all-zero matrix and identity matrix, respectively.

With the new notations we can express the real and imaginary terms of downlink SINR constraint in  $\mathcal{P}7$  as:

$$\text{Im}(\widetilde{\mathbf{h}}_i^H \mathbf{w}) = (\check{\mathbf{h}}_i + \Delta \widetilde{\mathbf{h}}_i) \underline{\mathbf{w}}, \quad \text{Re}(\widetilde{\mathbf{h}}_i^H \mathbf{w}) = (\check{\mathbf{h}}_i + \Delta \widetilde{\mathbf{h}}_i) \mathbf{\Pi} \underline{\mathbf{w}}. \quad (49)$$

From the definition of the error bound, we have  $\|\Delta \widetilde{\mathbf{h}}_i\|^2 \leq \epsilon_{h,i}^2$ , the downlink SINR constraint can be guaranteed by the following constraint

$$\begin{aligned} \max_{\|\Delta \widetilde{\mathbf{h}}_i\|^2 \leq \epsilon_{h,i}^2} & \left| (\check{\mathbf{h}}_i + \Delta \widetilde{\mathbf{h}}_i) \underline{\mathbf{w}} \right| \\ & - \left( (\check{\mathbf{h}}_i + \Delta \widetilde{\mathbf{h}}_i) \mathbf{\Pi} \underline{\mathbf{w}} - \sqrt{\Gamma_i^{DL} \sigma_i^2} \right) \tan \theta \leq 0, \quad \forall i. \end{aligned} \quad (50)$$

Hence, by considering the absolute value term, (50) is equivalent to the following two constraints

$$\begin{aligned} \max_{\|\Delta \widetilde{\mathbf{h}}_i\|^2 \leq \epsilon_{h,i}^2} & \check{\mathbf{h}}_i \underline{\mathbf{w}} + \Delta \widetilde{\mathbf{h}}_i \underline{\mathbf{w}} - (\check{\mathbf{h}}_i + \Delta \widetilde{\mathbf{h}}_i) \mathbf{\Pi} \underline{\mathbf{w}} \tan \theta \\ & + \sqrt{\Gamma_i^{DL} \sigma_i^2} \tan \theta \leq 0, \quad \forall i, \end{aligned} \quad (51)$$

$$\begin{aligned} \max_{\|\Delta \widetilde{\mathbf{h}}_i\|^2 \leq \epsilon_{h,i}^2} & -\check{\mathbf{h}}_i \underline{\mathbf{w}} - \Delta \widetilde{\mathbf{h}}_i \underline{\mathbf{w}} - (\check{\mathbf{h}}_i + \Delta \widetilde{\mathbf{h}}_i) \mathbf{\Pi} \underline{\mathbf{w}} \tan \theta \\ & + \sqrt{\Gamma_i^{DL} \sigma_i^2} \tan \theta \leq 0, \quad \forall i, \end{aligned} \quad (52)$$

whose robust formulations are given by

$$\begin{aligned} & \check{\mathbf{h}}_i \underline{\mathbf{w}} - \check{\mathbf{h}}_i \mathbf{\Pi} \underline{\mathbf{w}} \tan \theta + \epsilon_{h,i} \|\underline{\mathbf{w}} - \mathbf{\Pi} \underline{\mathbf{w}} \tan \theta\| \\ & + \sqrt{\Gamma_i^{DL} \sigma_i^2} \tan \theta \leq 0, \quad \forall i, \end{aligned} \quad (53)$$

$$\begin{aligned} & -\check{\mathbf{h}}_i \underline{\mathbf{w}} - \check{\mathbf{h}}_i \mathbf{\Pi} \underline{\mathbf{w}} \tan \theta + \epsilon_{h,i} \|-\underline{\mathbf{w}} - \mathbf{\Pi} \underline{\mathbf{w}} \tan \theta\| \\ & + \sqrt{\Gamma_i^{DL} \sigma_i^2} \tan \theta \leq 0, \quad \forall i. \end{aligned} \quad (54)$$

Next, we consider the uplink SINR constraint in problem  $\mathcal{P}7$ . Following equations (33) and (34) in Section V-A, the uplink SINR constraint can be rewritten as

$$\begin{aligned} & \frac{(\check{\mathbf{f}} + \Delta \widetilde{\mathbf{f}})^H \mathbf{Z}_j (\check{\mathbf{f}} + \Delta \widetilde{\mathbf{f}})}{|\mathbf{u}_j^H \check{\mathbf{G}} \mathbf{w} + \mathbf{u}_j^H \Delta \widetilde{\mathbf{G}} \mathbf{w}|^2 + \sigma_N^2 \|\mathbf{u}_j\|^2} \\ & \geq \Gamma_j^{UL}, \\ & \forall \|\Delta \mathbf{G}\|^2 \leq \epsilon_G^2, \quad \forall \|\Delta \widetilde{\mathbf{f}}\|^2 \leq \epsilon_{f,j}^2, \quad \forall j. \end{aligned} \quad (55)$$

We note that (55) can be guaranteed by the following constraints

$$\begin{aligned} \max_{\|\tilde{\Delta}\mathbf{f}\|^2 \leq \epsilon_f^2} & \left( \tilde{\mathbf{f}} + \tilde{\Delta}\mathbf{f} \right)^H \mathbf{Z}_j \left( \tilde{\mathbf{f}} + \tilde{\Delta}\mathbf{f} \right) - \Gamma_j^{UL} \left( c_j + \sigma_N^2 \|\mathbf{u}_j\|^2 \right) \\ & \geq 0, \quad \forall j, \end{aligned} \quad (56)$$

$$\max_{\|\Delta\mathbf{G}\|^2 \leq \epsilon_G^2} \left| \mathbf{u}_j^H \check{\mathbf{G}}\mathbf{w} + \mathbf{u}_j^H \Delta\mathbf{G}\mathbf{w} \right|^2 \leq c_j, \quad \forall j, \quad (57)$$

where  $c_j > 0, \forall j$ , are introduced as slack variables [46].

Similar procedure as in Section V-A can be applied to (56). By exploiting the S-procedure in Lemma 1, (56) can be expanded and converted into a LMI as shown below

$$\begin{aligned} \left[ \begin{array}{cc} \mu_j \mathbf{I}_N + \mathbf{Z}_j & \mathbf{Z}_j \tilde{\mathbf{f}} \\ \tilde{\mathbf{f}}^H \mathbf{Z}_j & \tilde{\mathbf{f}}^H \mathbf{Z}_j \tilde{\mathbf{f}} - \Gamma_j^{UL} c_j - \Gamma_j^{UL} \sigma_N^2 \text{Tr}(\mathbf{U}_j) - \mu_j \epsilon_f^2 \end{array} \right] \\ \geq 0, \quad \forall j. \end{aligned} \quad (58)$$

We note that by using the fact that  $\|\mathbf{x} + \mathbf{y}\|^2 \leq (\|\mathbf{x}\| + \|\mathbf{y}\|)^2$ , (57) can always be guaranteed by the following constraint

$$\max_{\|\Delta\mathbf{G}\|^2 \leq \epsilon_G^2} \left( |\mathbf{u}_j^H \check{\mathbf{G}}\mathbf{w}| + |\mathbf{u}_j^H \Delta\mathbf{G}\mathbf{w}| \right)^2 \leq c_j, \quad \forall j, \quad (59)$$

whose robust formulation is given by

$$\left( |\mathbf{u}_j^H \check{\mathbf{G}}\mathbf{w}| + \epsilon_G |\mathbf{u}_j^H \mathbf{w}| \right)^2 \leq c_j, \quad \forall j. \quad (60)$$

Futhermore, we define  $\underline{\mathbf{Y}}_j \triangleq \begin{bmatrix} \text{Re}(\mathbf{u}_j^H \check{\mathbf{G}}) & -\text{Im}(\mathbf{u}_j^H \check{\mathbf{G}}) \\ \text{Im}(\mathbf{u}_j^H \check{\mathbf{G}}) & \text{Re}(\mathbf{u}_j^H \check{\mathbf{G}}) \end{bmatrix}$  and  $\underline{\mathbf{U}}_j \triangleq \begin{bmatrix} \text{Re}(\mathbf{u}_j^H) & -\text{Im}(\mathbf{u}_j^H) \\ \text{Im}(\mathbf{u}_j^H) & \text{Re}(\mathbf{u}_j^H) \end{bmatrix}$ , thus, the constraint (60) can be written in terms of real valued numbers as

$$\left( |\underline{\mathbf{Y}}_j \mathbf{w}| + \epsilon_G |\underline{\mathbf{U}}_j \mathbf{w}| \right)^2 \leq c_j, \quad \forall j. \quad (61)$$

Therefore, the robust optimization problem based on CI is (62), shown at the bottom of this page. Note that problem  $\mathcal{P}8$  is jointly convex with respect to the optimization variables, thus can be optimally solved using standard convex solvers like CVX [43]. After we obtain the optimal  $\underline{\mathbf{w}}^*$  and  $P_j^*$ , the complex solution  $\mathbf{w}^*$  can be obtained from the relation in (45).

## VI. COMPUTATIONAL COMPLEXITY ANALYSIS

In this Section, we mathematically characterize the computational complexity of the conventional and proposed schemes based on MOOP formulations.

TABLE I

COMPLEXITY ANALYSIS OF THE MOOP FORMULATIONS

MOOP	Complexity Order
$\mathcal{P}1$ (SDP)	$O((KN^2 + J)[K(2 + N^3) + 2J + (KN^2 + J)(K(2 + N^2) + 2J) + KN^2 + (KN^2 + J)^2])$
$\tilde{\mathcal{P}}2$	$O((KN + J)[3J(1 + (KN + J)) + 2KN^2 + (KN + J)^2])$
$\mathcal{P}5$	$O((KN^2 + J)[K(N + 1)^2 + J(NJ + 1)^3 + J(N^2 + 1)^3 + J + KN^3 + (KN^2 + J)(K(N + 1)^2 + J(NJ + 1)^2 + J(N^2 + 1)^2 + J + KN^2) + (KN^2 + J)(KN^2) + (KN^2 + J)^2])$
$\mathcal{P}8$	$O((2N + J)[J(NJ + 1)^3 + J(N + 1)^3 + J + (2N + J)(J(NJ + 1)^2 + J + 12N^2) + (2N + J)^2])$

### A. Transmit Complexity

We note that the convex MOOP formulations  $\mathcal{P}1, \tilde{\mathcal{P}}2, \mathcal{P}5$  and  $\mathcal{P}8$  involve only LMI and second-order cone (SOC) constraints. As such, the problems can be solved by a standard interior-point method (IPM) [49]. Therefore we can use the worst-case runtime to analyse the complexity of the conventional and the proposed CI schemes.

Following [50], the complexity of a generic IPM for solving problems like  $\mathcal{P}1, \tilde{\mathcal{P}}2, \mathcal{P}5$  and  $\mathcal{P}8$  involve the computation of a per-optimization cost. In each iteration, the computation cost is dominated by (i) the formation of the coefficient matrix of the linear system, and (ii) the factorization of the coefficient matrix. The cost of formation of the coefficient ( $C_{form}$ ) matrix is on the order of

$$C_{form} = n \underbrace{\sum_{a=1}^A k_a^3 + n^2 \sum_{a=1}^A k_a^2}_{\text{due to the LMI}} + n \underbrace{\sum_{a=A+1}^B k_a^2}_{\text{due to the SOC}}$$

while the cost of factorizing ( $C_{fact}$ ) is on the order of  $C_{fact} = n^3$  ( $n$  = number of decision variables). Hence, the total computation cost per optimization is on the order of  $C_{form} + C_{fact}$  [50]. We assume for the sake of simplicity that the decision variables in  $\mathcal{P}1, \tilde{\mathcal{P}}2, \mathcal{P}5$  and  $\mathcal{P}8$  are real-valued.

Hence, using these concepts, we now analyse the computational complexity of  $\mathcal{P}1, \tilde{\mathcal{P}}2, \mathcal{P}5$  and  $\mathcal{P}8$ . First we consider SDP formulation of  $\mathcal{P}1$ , which has  $K$  LMI (trace) constraints of size 1, three  $J$  LMI (trace) constraints of size 1,  $K$  SOC constraints of size  $N$  and  $K$  LMI (trace) constraints of size  $N$ . Therefore, the complexity of the SDP formulation of  $\mathcal{P}1$  is

$$\begin{aligned} \mathcal{P}8: \min_{\underline{\mathbf{w}}, P_j, t} & t \\ \text{s.t. } & \tilde{\underline{\mathbf{h}}}_i \underline{\mathbf{w}} - \tilde{\underline{\mathbf{h}}}_i \mathbf{\Pi} \underline{\mathbf{w}} \tan \theta + \epsilon_{h,i} \|\underline{\mathbf{w}} - \mathbf{\Pi} \underline{\mathbf{w}} \tan \theta\| \leq \sqrt{\Gamma_i^{DL} \sigma_i^2} \tan \theta, \quad \forall i \\ & -\tilde{\underline{\mathbf{h}}}_i \underline{\mathbf{w}} - \tilde{\underline{\mathbf{h}}}_i \mathbf{\Pi} \underline{\mathbf{w}} \tan \theta + \epsilon_{h,i} \|\underline{\mathbf{w}} - \mathbf{\Pi} \underline{\mathbf{w}} \tan \theta\| \leq \sqrt{\Gamma_i^{DL} \sigma_i^2} \tan \theta, \quad \forall i, \\ & \left[ \begin{array}{cc} \mu_j \mathbf{I}_N + \mathbf{Z}_j & \mathbf{Z}_j \tilde{\mathbf{f}} \\ \tilde{\mathbf{f}}^H \mathbf{Z}_j & \tilde{\mathbf{f}}^H \mathbf{Z}_j \tilde{\mathbf{f}} - \Gamma_j^{UL} c_j - \Gamma_j^{UL} \sigma_N^2 \text{Tr}(\mathbf{U}_j) - \mu_j \epsilon_f^2 \end{array} \right] \geq 0, \quad \forall j, \\ & \left( |\underline{\mathbf{Y}}_j \underline{\mathbf{w}}| + \epsilon_G |\underline{\mathbf{U}}_j \underline{\mathbf{w}}| \right)^2 \leq c_j, \quad \forall j, \quad \lambda_a (R_a^* - R_a) \leq t, \quad \forall a \in \{1, 2\}, \quad \mu_j \geq 0, \quad c_j > 0, \quad \forall j. \end{aligned} \quad (62)$$

on the order shown in the first row of Table I. Similarly, we can determine the complexity order of the formulations  $\widetilde{\mathcal{P}}2$ ,  $\mathcal{P}5$  and  $\mathcal{P}8$  as shown in Table I, respectively. From Table I, we can show that the proposed MOOP formulation  $\widetilde{\mathcal{P}}2$  has lower complexity than the SDP formulation of  $\mathcal{P}1$  since it has lower order of variables to compute i.e lower cost of factorization ( $C_{fact}$ ). Also, we can straightforwardly show that for the robust MOOP, the proposed formulation  $\mathcal{P}8$  has a lower complexity than the conventional formulation  $\mathcal{P}5$  since  $\mathcal{P}5$  involves a more complicated set of constraints (5 LMI constraints and 1 SOC constraint). This is also consistent with our simulation results in the following Section.

At this point, we emphasize that as the MOOP formulations in  $\mathcal{P}1$  and  $\mathcal{P}5$  are data independent, they only need to be applied once during each channel coherence time. While as the proposed MOOP formulations in  $\widetilde{\mathcal{P}}2$  and  $\mathcal{P}8$  are data dependent, they need to be run on a symbol by symbol basis. In the following section we compare the resulting transmit complexity of conventional and proposed MOOP approaches for both slow and fast fading scenarios, and show that the average execution time per downlink frames is comparable for both techniques.

### B. Receiver Complexity

At the receiver side, for the case of the conventional beamforming, the downlink users in our FD system scenario need to equalize the composite channel  $\mathbf{h}_i^H \mathbf{w}_i^*$  to recover their data symbols, where  $\{\mathbf{w}_i^*\}_{i=1}^K$  is the optimal solution of  $\mathcal{P}1$ . For the case of the proposed CI scheme, since the received symbols already lie in the constructive region of the constellation as shown in Fig. 2 and Fig. 3, equalization is not required by the downlink users. This automatically translates to reduced complexity at the receiver. Accordingly, this implies that CSI is not required for detection at the downlink users for the proposed CI scheme. Thus, depending on the signaling and pilots already involved for the SINR estimation, the proposed CI scheme may lead to further savings in training time and overhead. Most importantly, this makes the proposed scheme resistant to any quantization errors from the CSI acquisition at the receiver.

## VII. SIMULATION RESULTS

In this section, we investigate the performance of our proposed system through simulations. We model all channels as independent and identically distributed Rayleigh fading for both the perfect and imperfect CSI cases. Systems with QPSK and 16QAM modulation are considered while it is clear that the benefit extends to any lower or higher order modulation. For comparison in every scenario, we compare the proposed technique, constructive interference (CI) with the conventional case i.e. when all interference is treated as harmful signal [32], [33]. We use  $N \times K \times J$  to denote an FD radio BS with  $N$  antennas,  $K$  downlink users and  $J$  uplink users, respectively.

### A. Uplink-Downlink Power Weighted Optimization

In Fig. 4, we investigate the weighted optimization between the downlink and uplink total transmit power for the case of

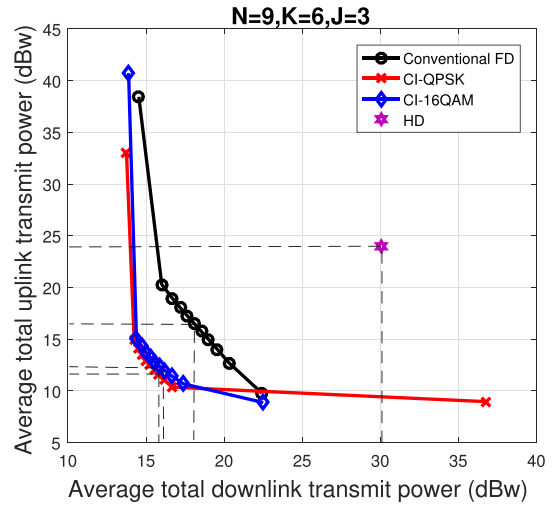


Fig. 4. Weighted optimization plot for the proposed scheme versus the conventional scheme  $N = 9$ ,  $K = 6$ ,  $J = 3$ .

$N = 9$ ,  $K = 6$ ,  $J = 3$  antennas. The plot is obtained by solving problem  $\mathcal{P}1$ ,  $\widetilde{\mathcal{P}}2$  and  $\mathcal{P}3$  for the conventional and CI cases, respectively, for  $0 \leq \lambda_a \leq 1$ ,  $a \in (1, 2)$  with a step size of 0.1. Note that  $\lambda_a$  determines the priority of the  $a$ -th objective. We assume the same required SINR for all downlink users to be  $\Gamma_i^{DL} = 15dB$ ,  $\Gamma_i^{UL} = 15dB$  for all uplink users, where  $\epsilon_G = 0.1$ . It can be seen from the plot that there is a trade-off between the two objectives (uplink and downlink) by varying the priority weight  $\lambda_a$ . We note that, although, the downlink transmit power is not directly dependent on the uplink transmit power, this trade-off is as a result of the link between the downlink and uplink transmit power through the SI term. In addition, we would like to emphasize the usefulness of the uplink and downlink SINR constraints in the optimizations to ensure the required QoS is achieved even in critical scenarios such as when the uplink power is low or the SI is high. Thus, for comparison, making reference to the point when  $\lambda_a = 0.5$  as indicated by the dotted lines, we can observe that the CI scheme has power savings of 4dB and 2.8dB for uplink and downlink users, respectively, for QPSK modulation. Accordingly, for 16QAM modulation, we can observe power savings of 3.5dB and 2.5dB for uplink and downlink users, respectively. Note that the proposed schemes are only outperformed by the conventional beamforming for the case  $\lambda_1 = 0$ ,  $\lambda_2 = 1$ , where all priority is given to the uplink PM problem, where interference exploitation does not apply. The figure also depicts the performance of a HD system as a reference. Here the total uplink and downlink data rate of HD is set equal to the one for FD, which requires that the individual uplink and downlink data rate requirements are double the ones for the FD case, due to the slotted HD transmission. It can be seen that the HD operation results in increased uplink and downlink power to achieve the same total rate, which highlights the effectiveness of the FD approach.

In Fig. 5, we plot the case when we have  $N = 8$ ,  $K = 6$ ,  $J = 3$ . The same trend can be seen with Fig. 4, where we have when  $\lambda_a = 0.5$ , as indicated by the dotted lines, for QPSK modulation power savings of about 9dB and

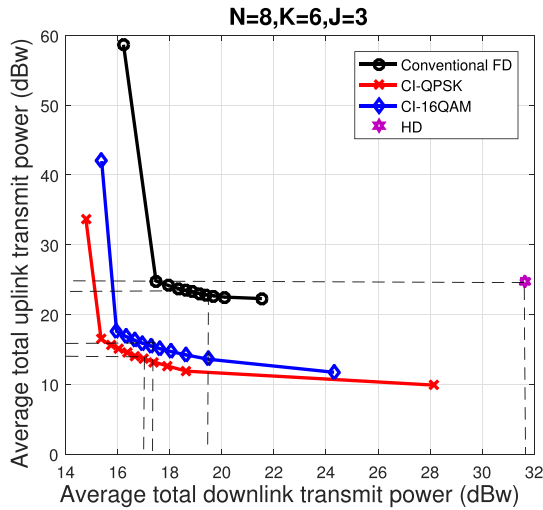


Fig. 5. Weighted optimization plot for the proposed scheme versus the conventional scheme  $N = 8, K = 6, J = 3$ .

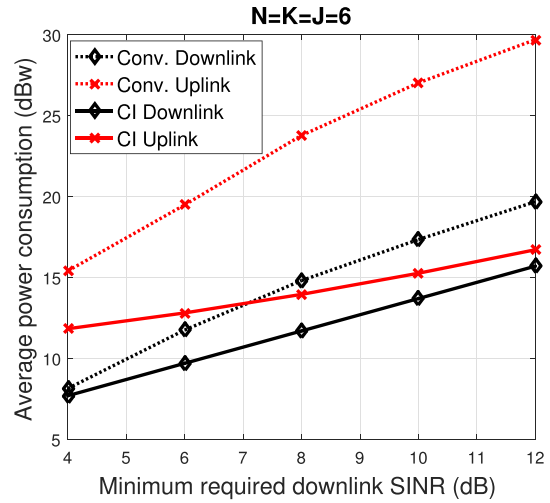


Fig. 7. Average power consumption versus minimum required downlink SINR when  $\lambda_1 = 0.9, \lambda_2 = 0.1, \epsilon_G = 0.1$  and  $\Gamma^{UL} = 0\text{dB}$  for QPSK modulation.

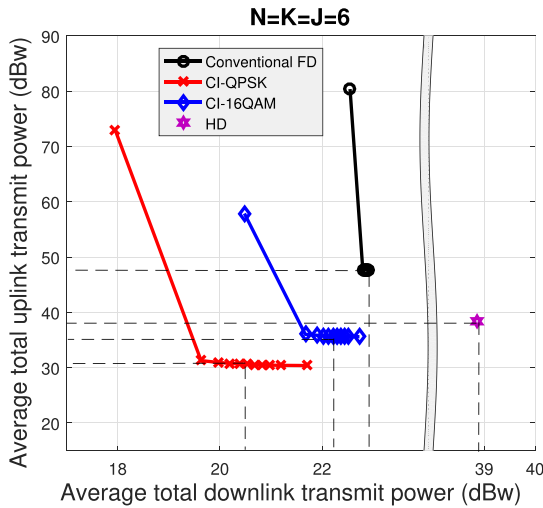


Fig. 6. Weighted optimization plot for the proposed scheme versus the conventional scheme  $N = 6, K = 6, J = 6$ .

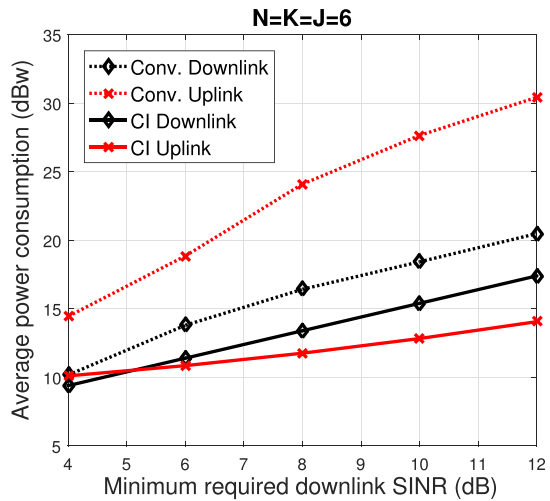


Fig. 8. Average power consumption versus minimum required downlink SINR when  $\lambda_1 = 0.1, \lambda_2 = 0.9, \epsilon_G = 0.1$  and  $\Gamma^{UL} = 0\text{dB}$  for QPSK modulation.

2.1dB for the uplink and downlink users, respectively. For 16QAM modulation, we have power savings of about 7.5dB and 1.6dB for the uplink and downlink users, respectively. Again, it can be seen that the FD transmission outperforms the HD benchmark. Fig. 4 shows the scenario when the number of antennas at the FD BS is equal to the total number of uplink and downlink users, while Fig. 5 shows the scenario when there is one less antenna at the FD BS to serve the uplink and downlink users. This implies a lower degree of freedom compared to the scenario in Fig. 4, and is in fact a critical scenario where conventional approaches break down and lead to highly inefficient solutions. Thus, leading to increased uplink and downlink power consumption compared to the CI scheme.

In Fig. 6, we show a scenario where we have equal number of antennas at the FD radio BS and at the users  $N = K = J = 6$ . With this setup, when  $\lambda_a = 0.5$ , we can see for QPSK modulation uplink and downlink user power savings

of about 17dB and 2.4dB, respectively, and about 12.1dB and 0.8dB, respectively. The reason is because for  $N = K = J = 6$  the problem is more restricted in the optimization variable dimensions and the conventional scheme in this scenario leads to greatly increased uplink and downlink powers while for the CI scheme this scenario can be accommodated and has higher feasibility so consumes lower power. Again, it can be observed that the FD transmission outperforms the HD benchmark. These results highlight a key advantage of the proposed scheme over the conventional approaches.

### B. Average Transmit Power Versus Minimum Required SINR

In Fig. 7 and Fig. 8, we investigate the power consumption of the downlink and uplink users for different minimum required downlink SINR ( $\Gamma_i^{DL}$ ). For both plots we assume a minimum required uplink SINR  $\Gamma_j^{UL} = 0\text{dB}$  for all uplink

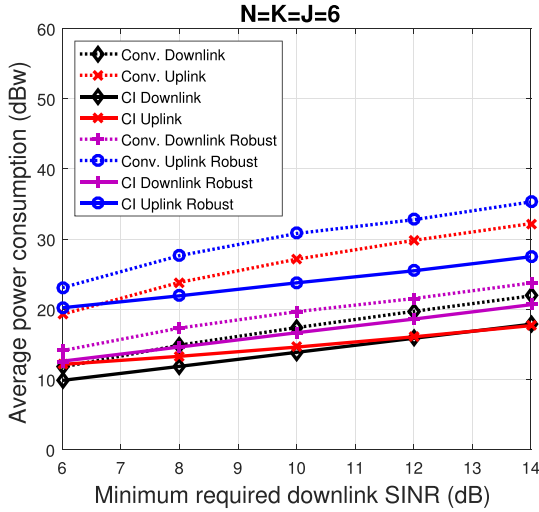


Fig. 9. Average power consumption versus minimum required downlink SINR when  $\lambda_1 = 0.9$ ,  $\lambda_2 = 0.1$ ,  $\Gamma^{UL} = 0\text{dB}$  and  $\epsilon_h = \epsilon_f = \epsilon_G = 0.1$  for QPSK modulation.

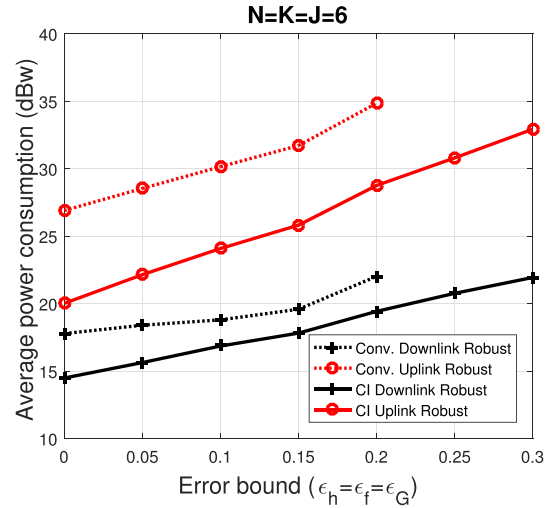


Fig. 10. Average power consumption versus error bounds when  $\lambda_1 = 0.9$ ,  $\lambda_2 = 0.1$ ,  $\Gamma^{UL} = 0\text{dB}$  and  $\Gamma^{DL} = 10\text{dB}$  for QPSK modulation.

users. In Fig. 7, we select  $\lambda_1 = 0.9$  and  $\lambda_2 = 0.1$ , which gives higher priority to the total downlink transmit power minimization problem. It can be observed that both the uplink and downlink power consumption increases with increase in  $\Gamma_i^{DL}$ . This is because an increase in the downlink SINR requirement translates to increase in downlink transmit power and hence increase in the SI power. Therefore, the uplink users have to transmit with a higher power to meet their QoS requirement ( $\Gamma_j^{UL}$ ). However, we can still see power savings of up to 12dB and 4dB for the uplink and downlink users, respectively, for the CI scheme compared to the conventional scheme. Also, we note that while CI is applied to only the downlink users, more power is saved for the uplink users than the downlink users. This is because with CI the total downlink transmit power is reduced and this directly reduces the residual SI power at the FD BS. Accordingly, the constructive interference power has been traded off for both uplink and downlink power savings. The same trend can be seen in the Fig. 8, where  $\lambda_1 = 0.1$  and  $\lambda_2 = 0.9$ . It can be observed that in this scenario since we give higher priority to the uplink power minimization problem, we have higher power savings for the uplink users and lower power savings for the downlink users compared to the Fig. 7.

### C. MOOP with Imperfect CSI

In Fig. 9 and 10, we investigate the performance of the proposed CSI-robust CI scheme for  $N = K = J = 6$ , we select  $\lambda_1 = 0.9$  and  $\lambda_2 = 0.1$ . Fig. 9 shows the Average power consumption for the uplink and downlink users when the error bounds  $\epsilon_h = \epsilon_f = \epsilon_G = 0.1$ . It can be seen that the CI scheme shows better performance than the conventional scheme with power savings of 8dB and 3dB for the uplink and downlink users, respectively. This is also shown in Fig. 10, which shows the average power consumption with increasing error bounds. It can be seen that feasible solutions can only be found for  $\epsilon_h = \epsilon_f = \epsilon_G \leq 0.2$ . Besides, even if feasible results

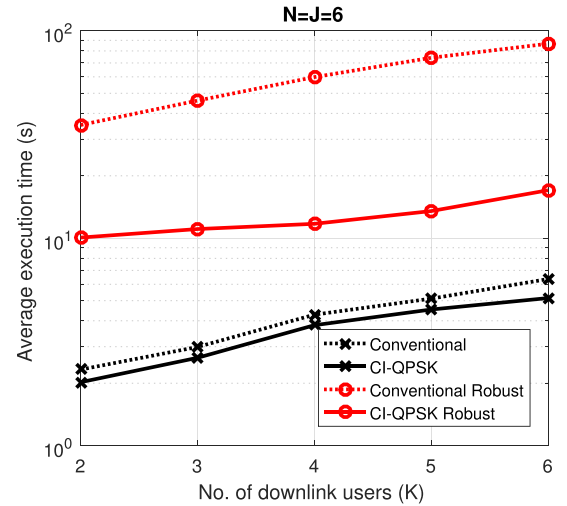


Fig. 11. Average execution time per optimization versus number of downlink users with  $N = J = 6$  when  $\lambda_1 = 0.9$ ,  $\lambda_2 = 0.1$ ,  $\Gamma^{UL} = 0\text{dB}$ ,  $\Gamma^{DL} = 5\text{dB}$  and  $\epsilon_h = \epsilon_f = \epsilon_G = 0.01$ .

could be found, significant amount of power will be consumed as can be seen for error bound values between 0.15 and 0.2 for both uplink and downlink users.

### D. Complexity

In Fig. 11, we compare the Average execution time per optimization of the conventional scheme and the proposed CI scheme for different number of downlink users ( $K$ ) with  $N = J = 6$ . We fixed  $\lambda_1 = 0.9$ ,  $\lambda_2 = 0.1$ ,  $\Gamma^{UL} = 0\text{dB}$ ,  $\Gamma^{DL} = 5\text{dB}$  and  $\epsilon_h = \epsilon_f = \epsilon_G = 0.01$ . This plot shows the complexity comparison of the proposed and conventional schemes in terms of average execution time. This is computed by generating  $K$  random QPSK symbols for 100,000 channel realizations. Thus, taking into consideration 100,000 random symbol combinations over 100,000 iterations. We kindly want to emphasize that the execution time is not only dependent on the symbol combinations, but also on the channel realization

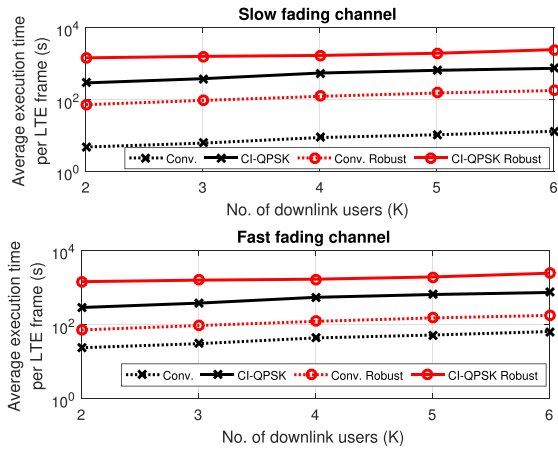


Fig. 12. Average execution time versus number of downlink users for slow/fast fading channels with  $N = J = 6$  when  $\lambda_1 = 0.9$ ,  $\lambda_2 = 0.1$ ,  $\Gamma^{UL} = 0\text{dB}$ ,  $\Gamma^{DL} = 5\text{dB}$  and  $\epsilon_h = \epsilon_f = \epsilon_G = 0.01$ .

and the problem formulation, i.e. the geometry and number of constraints, stemming from the number of users, antennas, e.t.c. It can be seen that for the perfect CSI case, the proposed CI scheme takes 83% of time taken by the conventional scheme. While for the imperfect CSI case, the proposed CI scheme takes about 28% of the time taken by the conventional scheme. This is because the conventional approach involves a more complicated set of constraints, hence, more computational cost as shown in Section VI-A above. Besides, the proposed MOOP ( $\mathcal{P}_8$ ) formulation involves a multicast approach which reduces the number variables to compute.

As we have noted above however, the proposed data dependent optimization needs to be run on a symbol-by-symbol basis. To obtain a fairer comparison, we plot in Fig. 12 the average execution time per frame versus the number of downlink users for slow and fast fading channels. Here, we assume the LTE Type 2 TDD frame structure [51], where each frame is subdivided to 10 subframes each with a duration  $1\text{ms}$  and containing 14 symbol-time slots. Accordingly, we assume that for fast fading the channel is constant for the duration of a subframe with a number of symbols per coherence time  $N_{coh} = 14$ , while for slow fading we assume a coherence time equal to 5 subframes with  $N_{coh} = 70$  [51]. The results for both slow and fast fading channels show the end complexity of the proposed CI approaches are comparable to those with the conventional approaches. Accordingly, and in conjunction with the performance improvements shown in the previous results, it can be seen that the proposed schemes provide a much more favorable performance complexity trade-off w.r.t. conventional interference mitigation.

## VIII. CONCLUSION

In this paper we studied the application of the interference exploitation concept to a MU-MIMO system with a FD radio BS. The optimization problem was formulated as a convex Multi-Objective optimization problem (MOOP) via the weighted Tchebycheff method. The MOOP was formulated for both PSK and QAM modulations by adapting the decision

thresholds in both cases to accommodate for constructive interference. The CI scheme was also extended to robust designs for imperfect downlink and uplink CSI with bounded CSI errors. Simulation results proved the significant power savings of the CI scheme over the conventional scheme in every scenario. More importantly, we have shown that through the FD MOOP formulation, constructive interference power can be traded off for both uplink and downlink power savings.

## ACKNOWLEDGMENT

The author would like to thank the Federal Republic of Nigeria and the Petroleum Technology Development Fund (PTDF) for funding the Ph.D. course.

## REFERENCES

- [1] V. W. S. Wong, R. Schober, D. W. K. Ng, and L.-C. Wang, Eds., *Key Technologies for 5G Wireless Systems*. Cambridge, U.K.: Cambridge Univ. Press, 2017.
- [2] D. Bharadia, E. McMillin, and S. Katti, "Full duplex radios," *ACM SIGCOMM Comput. Commun. Rev.*, vol. 43, no. 4, pp. 375–386, 2013.
- [3] J. I. Choi, M. Jain, K. Srinivasan, P. Levis, and S. Katti, "Achieving single channel, full duplex wireless communication," in *Proc. 16th Annu. Int. Conf. Mobile Comput. Netw.*, 2010, pp. 1–12.
- [4] D. Nguyen, L.-N. Tran, P. Pirinen, and M. Latva-Aho, "On the spectral efficiency of full-duplex small cell wireless systems," *IEEE Trans. Wireless Commun.*, vol. 13, no. 9, pp. 4896–4910, Sep. 2014.
- [5] H. Q. Ngo, H. A. Suraweera, M. Matthaiou, and E. G. Larsson, "Multipair full-duplex relaying with massive arrays and linear processing," *IEEE J. Sel. Areas Commun.*, vol. 32, no. 9, pp. 1721–1737, Sep. 2014.
- [6] M. H. M. Costa, "Writing on dirty paper (corresp.)," *IEEE Trans. Inf. Theory*, vol. 29, no. 5, pp. 439–441, May 1983.
- [7] C. Masouros, M. Sellathurai, and T. Ratnarajah, "Interference optimization for transmit power reduction in Tomlinson-Harashima precoded MIMO downlinks," *IEEE Trans. Signal Process.*, vol. 60, no. 5, pp. 2470–2481, May 2012.
- [8] A. Garcia-Rodriguez and C. Masouros, "Power-efficient Tomlinson-Harashima precoding for the downlink of multi-user MISO systems," *IEEE Trans. Commun.*, vol. 62, no. 6, pp. 1884–1896, Jun. 2014.
- [9] C. B. Peel, B. M. Hochwald, and A. L. Swindlehurst, "A vector-perturbation technique for near-capacity multiantenna multiuser communication—Part I: Channel inversion and regularization," *IEEE Trans. Commun.*, vol. 53, no. 1, pp. 195–202, Jan. 2005.
- [10] C. Masouros and E. Alsusa, "Dynamic linear precoding for the exploitation of known interference in MIMO broadcast systems," *IEEE Trans. Wireless Commun.*, vol. 8, no. 3, pp. 1396–1404, Mar. 2009.
- [11] C. Masouros, "Correlation rotation linear precoding for MIMO broadcast communications," *IEEE Trans. Signal Process.*, vol. 59, no. 1, pp. 252–262, Jan. 2011.
- [12] M. Bengtsson and B. Ottersten, "Handbook of antennas in wireless communications," in *Optimal and Suboptimal Transmit Beamforming*. Boca Raton, FL, USA: CRC Press, 2001.
- [13] G. Zheng, K.-K. Wong, and T.-S. Ng, "Robust linear MIMO in the downlink: A worst-case optimization with ellipsoidal uncertainty regions," *EURASIP J. Adv. Signal Process.*, vol. 2008, p. 609028, Jul. 2008.
- [14] M. Schubert and H. Boche, "Solution of the multiuser downlink beamforming problem with individual SINR constraints," *IEEE Trans. Veh. Technol.*, vol. 53, no. 1, pp. 18–28, Jan. 2004.
- [15] C. Masouros, M. Sellathurai, and T. Ratnarajah, "Vector perturbation based on symbol scaling for limited feedback MISO downlinks," *IEEE Trans. Signal Process.*, vol. 62, no. 3, pp. 562–571, Feb. 2014.
- [16] C. Masouros, T. Ratnarajah, M. Sellathurai, C. B. Papadias, and A. Shukla, "Known interference in the cellular downlink: A performance limiting factor or a source of green signal power?" *IEEE Commun. Mag.*, vol. 51, no. 10, pp. 162–171, Oct. 2013.
- [17] G. Zheng, I. Krikidis, C. Masouros, S. Timotheou, D.-A. Toumpakaris, and Z. Ding, "Rethinking the role of interference in wireless networks," *IEEE Commun. Mag.*, vol. 52, no. 11, pp. 152–158, Nov. 2014.
- [18] M. Alodeh, S. Chatzinotas, and B. Ottersten, "Constructive multiuser interference in symbol level precoding for the MISO downlink channel," *IEEE Trans. Signal Process.*, vol. 63, no. 9, pp. 2239–2252, May 2015.

- [19] M. Alodeh, S. Chatzinotas, and B. Ottersten, "Symbol-level multiuser MISO precoding for multi-level adaptive modulation," *IEEE Trans. Signal Process.*, vol. 16, no. 8, pp. 5511–5524, Aug. 2017.
- [20] M. Alodeh, S. Chatzinotas, and B. Ottersten, "Energy-efficient symbol-level precoding in multiuser MISO based on relaxed detection region," *IEEE Trans. Wireless Commun.*, vol. 15, no. 5, pp. 3755–3767, May 2016.
- [21] C. Masouros and G. Zheng, "Exploiting known interference as green signal power for downlink beamforming optimization," *IEEE Trans. Signal Process.*, vol. 63, no. 14, pp. 3628–3640, Jul. 2015.
- [22] K. L. Law, C. Masouros, and M. Pesavento, "Transmit precoding for interference exploitation in the underlay cognitive radio Z-channel," *IEEE Trans. Signal Process.*, vol. 65, no. 14, pp. 3617–3631, Jul. 2017.
- [23] A. Li and C. Masouros, "Exploiting constructive mutual coupling in P2P MIMO by analog-digital phase alignment," *IEEE Trans. Wireless Commun.*, vol. 16, no. 3, pp. 1948–1962, Mar. 2017.
- [24] P. V. Amadori and C. Masouros, "Constant envelope precoding by interference exploitation in phase shift keying-modulated multiuser transmission," *IEEE Trans. Wireless Commun.*, vol. 16, no. 1, pp. 538–550, Jan. 2017.
- [25] P. V. Amadori and C. Masouros, "Interference-driven antenna selection for massive multiuser MIMO," *IEEE Trans. Veh. Technol.*, vol. 65, no. 8, pp. 5944–5958, Aug. 2016.
- [26] P. V. Amadori and C. Masouros, "Large scale antenna selection and precoding for interference exploitation," *IEEE Trans. Commun.*, vol. 65, no. 10, pp. 4529–4542, Oct. 2017.
- [27] S. Timotheou, G. Zheng, C. Masouros, and I. Krikidis, "Exploiting constructive interference for simultaneous wireless information and power transfer in multiuser downlink systems," *IEEE J. Sel. Areas Commun.*, vol. 34, no. 5, pp. 1772–1784, May 2016.
- [28] M. R. A. Khandaker, C. Masouros, and K.-K. Wong, "Constructive interference based secure precoding: A new dimension in physical layer security," *IEEE Trans. Inf. Forensics Security*, vol. 13, no. 9, pp. 2256–2268, Sep. 2018.
- [29] F. Liu, C. Masouros, A. Li, T. Ratnarajah, and J. Zhou, "Interference exploitation for radar and cellular coexistence—The power-efficient approach," in *Proc. 5th Colloq. Antennas, Wireless Electromagn.*, 2017, pp. 1–23.
- [30] A. Li and C. Masouros, "Interference exploitation precoding made practical: Optimal closed-form solutions for PSK modulations," *IEEE Trans. Wireless Commun.*, to be published, doi: [10.1109/TWC.2018.2869382](https://doi.org/10.1109/TWC.2018.2869382).
- [31] A. Li, C. Masouros, F. Liu, and A. L. Swindlehurst, "Massive MIMO 1-bit DAC transmission: A low-complexity symbol scaling approach," *IEEE Trans. Wireless Commun.*, to be published, doi: [10.1109/TWC.2018.2868369](https://doi.org/10.1109/TWC.2018.2868369).
- [32] Y. Sun, D. W. K. Ng, and R. Schober, "Multi-objective optimization for power efficient full-duplex wireless communication systems," in *Proc. IEEE Global Commun. Conf. (GLOBECOM)*, Dec. 2015, pp. 1–6.
- [33] Y. Sun, D. W. K. Ng, J. Zhu, and R. Schober, "Multi-objective optimization for robust power efficient and secure full-duplex wireless communication systems," *IEEE Trans. Wireless Commun.*, vol. 15, no. 8, pp. 5511–5526, Aug. 2016.
- [34] S. Leng, D. W. K. Ng, N. Zlatanov, and R. Schober, "Multi-objective resource allocation in full-duplex SWIPT systems," in *Proc. IEEE Int. Conf. Commun. (ICC)*, May 2016, pp. 1–7.
- [35] H. Min, J. Lee, S. Park, and D. Hong, "Capacity enhancement using an interference limited area for device-to-device uplink underlying cellular networks," *IEEE Trans. Wireless Commun.*, vol. 10, no. 12, pp. 3995–4000, Dec. 2011.
- [36] M. Ni, L. Zheng, F. Tong, J. Pan, and L. Cai, "A geometrical-based throughput bound analysis for device-to-device communications in cellular networks," *IEEE J. Sel. Areas Commun.*, vol. 33, no. 1, pp. 100–110, Jan. 2015.
- [37] Y. Feng, X. Shen, R. Zhang, and P. Zhou, "Interference-area-based resource allocation for full-duplex communications," in *Proc. IEEE Int. Conf. Commun. Syst. (ICCS)*, Dec. 2016, pp. 1–5.
- [38] H. Zhang, Y. Liao, and L. Song, "D2D-U: Device-to-device communications in unlicensed bands for 5G system," *IEEE Trans. Wireless Commun.*, vol. 16, no. 6, pp. 3507–3519, Jun. 2017.
- [39] D. Bharadia and S. Katti, "Full duplex MIMO radios," in *Proc. USENIX NSDI*, 2014, pp. 359–372.
- [40] B. P. Day, A. R. Margetts, D. W. Bliss, and P. Schniter, "Full-duplex MIMO relaying: Achievable rates under limited dynamic range," *IEEE J. Sel. Areas Commun.*, vol. 30, no. 8, pp. 1541–1553, Sep. 2012.
- [41] B. Li, H. H. Dam, A. Cantoni, and K. L. Teo, "Some interesting properties for zero-forcing beamforming under per-antenna power constraints in rural areas," *J. Global Optim.*, vol. 62, no. 4, pp. 877–886, 2015.
- [42] R. T. Marler and J. S. Arora, "Survey of multi-objective optimization methods for engineering," *Struct. Multidiscipl. Optim.*, vol. 26, no. 6, pp. 369–395, Apr. 2004.
- [43] M. Grant, S. Boyd, and Y. Ye. (2015). *CVX: Matlab Software for Disciplined Convex Programming (2008)*. [Online]. Available: <http://stanford.edu/boyd/cvx>
- [44] M. Alodeh, S. Chatzinotas, and B. Ottersten, "Constructive interference through symbol level precoding for multi-level modulation," in *Proc. IEEE Global Commun. Conf. (GLOBECOM)*, Dec. 2015, pp. 1–6.
- [45] N. Vucic and H. Boche, "Robust QoS-constrained optimization of downlink multiuser MISO systems," *IEEE Trans. Signal Process.*, vol. 57, no. 2, pp. 714–725, Feb. 2009.
- [46] S. Boyd and L. Vandenberghe, *Convex Optimization*. Cambridge, U.K.: Cambridge Univ. Press, 2004.
- [47] W.-K. Ma, J. Pan, A. M.-C. So, and T.-H. Chang, "Unraveling the rank-one solution mystery of robust MISO downlink transmit optimization. A verifiable sufficient condition via a new duality result," *IEEE Trans. Signal Process.*, vol. 65, no. 7, pp. 1909–1924, Apr. 2017.
- [48] Z.-Q. Luo, W.-K. Ma, A. M.-C. So, Y. Ye, and S. Zhang, "Semidefinite relaxation of quadratic optimization problems," *IEEE Signal Process. Mag.*, vol. 27, no. 3, pp. 20–34, May 2010.
- [49] A. Ben-Tal and A. Nemirovski, *Lectures on Modern Convex Optimization: Analysis, Algorithms, and Engineering Applications*. Philadelphia, PA, USA: SIAM, 2001.
- [50] K.-Y. Wang, A. Man-Cho So, T.-H. Chang, W.-K. Ma, and C.-Y. Chi, "Outage constrained robust transmit optimization for multiuser MISO downlinks: Tractable approximations by conic optimization," *IEEE Trans. Signal Process.*, vol. 62, no. 21, pp. 5690–5705, Nov. 2014.
- [51] *Evolved Universal Terrestrial Radio Access (E-UTRA); LTE Physical Layer; General Description*, document 3GPP TS 36.201 V11.1.0 Release 11, 2013.



**Mahmoud T. Kabir** (S'17) received the bachelor's degree in electrical and electronic engineering from the University of Sussex, U.K., in 2012, and the master's degree in communication engineering from The University of Manchester, U.K., in 2013. He is currently pursuing the Ph.D. degree with the Communications and Information Systems Research Group, Department of Electronic and Electrical Engineering, University College London, U.K. His research interests include precoding designs for MIMO systems, full-duplex systems, and convex optimization.



**Muhammad R. A. Khandaker** (S'10–M'13–SM'18) received the B.Sc. degree (Hons.) in computer science and engineering from Jahangirnagar University, Dhaka, Bangladesh, in 2006, the M.Sc. degree in telecommunications engineering from East West University, Dhaka, in 2007, and the Ph.D. degree in electrical and computer engineering from Curtin University, Australia, in 2013.

He held a number of academic positions in Bangladesh. He was a Post-Doctoral Researcher with the Department of Electronic and Electrical Engineering, University College London, U.K., from 2013 to 2018. He is currently an Assistant Professor with the School of Engineering and Physical Sciences, Heriot-Watt University, U.K. He received the Curtin International Postgraduate Research Scholarship for the Ph.D. degree in 2009. He was a recipient of the Best Paper Award from the 16th IEEE Asia-Pacific Conference on Communications, Auckland, New Zealand, in 2010. He also served as the Managing Guest Editor for *Physical Communication* (Elsevier), Special Issue on Self-Optimizing Cognitive Radio Technologies. He is an Associate Editor for the IEEE ACCESS and the *EURASIP Journal on Wireless Communications and Networking*. He is currently serving as the Lead Guest Editor for the *EURASIP Journal on Wireless Communications and Networking*, Special Issue on Heterogeneous Cloud Radio Access Networks.



**Christos Masouros** (S'10–M'13–SM'18) received the Diploma degree in electrical and computer engineering from the University of Patras, Greece, in 2004, and the M.Sc. and the Ph.D. degrees in electrical and electronic engineering from The University of Manchester, U.K., in 2006 and 2009, respectively. In 2008, he was a Research Intern with Philips Research Labs, U.K., From 2009 to 2010, he was a Research Associate with The University of Manchester. In 2012, he was a Research Fellow with Queen's University Belfast. In 2012, he joined

the University College London as a Lecturer. He was a recipient of the Royal Academy of Engineering Research Fellowship from 2011 to 2016.

He is currently an Associate Professor with the Communications and Information Systems Research Group, Department of Electrical and Electronic Engineering, University College London. His research interests lie in the

fields of wireless communications and signal processing with a particular focus on green communications, large-scale antenna systems, cognitive radio, and interference mitigation techniques for MIMO and multicarrier communications. He is currently an Elected Member of the EURASIP SAT Committee on Signal Processing for Communications and Networking. He is also a member of the IET. He was a recipient of the Best Paper Award from the IEEE GLOBECOM 2015 Conference. He was recognized as an Exemplary Editor of the IEEE COMMUNICATIONS LETTERS and the IEEE TRANSACTIONS ON COMMUNICATIONS. He was a Guest Editor of the IEEE JOURNAL ON SELECTED TOPICS IN SIGNAL PROCESSING, Special Issues on Exploiting Interference Towards Energy Efficient and Secure Wireless Communications and Hybrid Analog/Digital Signal Processing for Hardware-Efficient Large Scale Antenna Arrays. He is currently an Editor for the IEEE TRANSACTIONS ON COMMUNICATIONS and an Associate Editor for the IEEE COMMUNICATIONS LETTERS.